

藏东义敦地体早古生代构造格局:来自碎屑锆石 U-Pb-Hf 同位素的约束

田振东¹⁾, 冷成彪^{2,3)}, 郭剑衡⁴⁾, 张兴春^{*1)}, 田丰⁵⁾, 马荣林¹⁾

1) 中国科学院地球化学研究所矿床地球化学国家重点实验室, 贵州贵阳, 550081;

2) 东华理工大学核资源与环境国家重点实验室, 江西南昌, 330013;

3) 东华理工大学地球科学学院, 江西南昌, 330013; 4) 苏州经贸职业技术学院, 江苏苏州, 215009;

5) 湖北省地质局冶金地质勘探大队, 湖北十堰, 442000

内容提要:位于藏东的义敦地体是研究青藏高原和古特提斯构造演化的关键区域, 其在早古生代时期的古地理位置及构造演化过程尚不明确。沉积岩中碎屑锆石记录了物源区丰富的地质信息, 被广泛应用于示踪沉积物源和古地理重建。本文对义敦地体三件下古生界浅变质沉积岩样品开展了碎屑锆石 LA-ICP-MS U-Pb 年代学和 Hf 同位素研究, 结果显示:三件样品均具有“多峰”的碎屑锆石年龄分布特征, 其 U-Pb 年龄主要集中在约 2535~2350 Ma、约 1000~900 Ma、约 890~750 Ma 和约 590~520 Ma 四个区间, 对应的 $\epsilon_{\text{Hf}}(t)$ 值分别为 -8.8~13.1、-11.8~10.0、-20.1~12.6 和 -27.6~6.1。综合本次研究结果和前人数据, 提出义敦地体下古生界变沉积岩中约 2535~2350 Ma 和约 890~750 Ma 年龄段的锆石主要来自邻区松潘-甘孜地体和华南地块, 而约 1000~900 Ma 和约 590~520 Ma 年龄段的碎屑锆石主要源自东冈瓦纳大陆 Rayner-Eastern Ghats、Prydz-Darling 和 Kuunga 造山带的岩浆岩。对比该地层与区内新元古界碎屑岩及相邻地体下古生界碎屑岩沉积物源在时空上的异同, 提出义敦地体可能于埃迪卡拉纪晚期—早寒武世(570~520 Ma)与印度地块发生拼合, 成为冈瓦纳大陆的一部分。在早古生代, 义敦地体可能位于东冈瓦纳大陆的北缘, 邻近羌塘和特提斯喜马拉雅地体。

关键词:义敦地体;恰斯群;沉积物源;碎屑锆石;构造演化

青藏高原是全球海拔最高、最年轻的高原, 也是目前正在活动中的大陆碰撞区, 其形成与演化以及高原隆升对东亚气候环境的影响是当前国内外地学研究的热点(Yin et al., 2000; 许志琴等, 2016; Grocholski, 2019)。大量证据表明, 现今的青藏高原是自早古生代以来由多个从冈瓦纳大陆裂解的地体(或微陆块)依次拼贴在欧亚大陆的南缘而形成, 期间依次经历了原特提斯、古特提斯、中特提斯、新特提斯洋的诞生、生长和消亡等过程(Pan Guitang et al., 2012; Metcalfe, 2021), 查清其内部各地体的地质演化过程对重建整个青藏高原的演化历史具

有重要意义。近年来, 国内外学者集中对拉萨、羌塘等构成青藏高原的主要地体的构造属性和演化过程开展了深入研究(Ma Anlin et al., 2017; Hu Peiyuan et al., 2019), 但是对一些规模较小地体(尤其是义敦地体)的相关研究则明显缺乏, 这在一定程度限制了人们对青藏高原构造演化过程的深入认识。

义敦地体位于青藏高原东缘, 呈“反 S”形夹持于羌塘地体、松潘-甘孜地体和扬子地块之间(图 1), 是研究青藏高原和古特提斯构造演化最为有利的地区之一。在晚三叠世, 甘孜-理塘古特提斯洋向

注:本文为国家自然科学基金项目(编号 42102277、41872097), 第二次青藏高原科学综合科学考察研究项目(编号 2021QZKK0301), 博士后基金(编号 2021 M703188)联合资助成果。

收稿日期:2022-09-19; 改回日期:2023-01-24; 网络发表日期:2023-03-16; 责任编辑:周健。

作者简介:田振东,男,1992 年生,博士后。E-mail:1345733476@qq.com。

* 通讯作者:张兴春,男,1964 年生。研究员,博士生导师,主要从事岩浆热液矿床成矿理论与找矿方法研究。E-mail: zhangxingchun@vip.gyig.ac.cn。

引用本文:田振东,冷成彪,郭剑衡,张兴春,田丰,马荣林. 2023. 藏东义敦地体早古生代构造格局:来自碎屑锆石 U-Pb-Hf 同位素的约束. 地质学报, 97(4): 1088~1105, doi: 10.19762/j.cnki.dizhixuebao.2023222.

Tian Zhendong, Leng Chengbiao, Guo Jianheng, Zhang Xingchun, Tian Feng, Ma Ronglin. 2023. Early Paleozoic tectonic framework of the Yidun Terrane, eastern Tibetan Plateau: Constraints from detrital zircon U-Pb-Hf isotopic compositions. Acta Geologica Sinica, 97(4): 1088~1105.

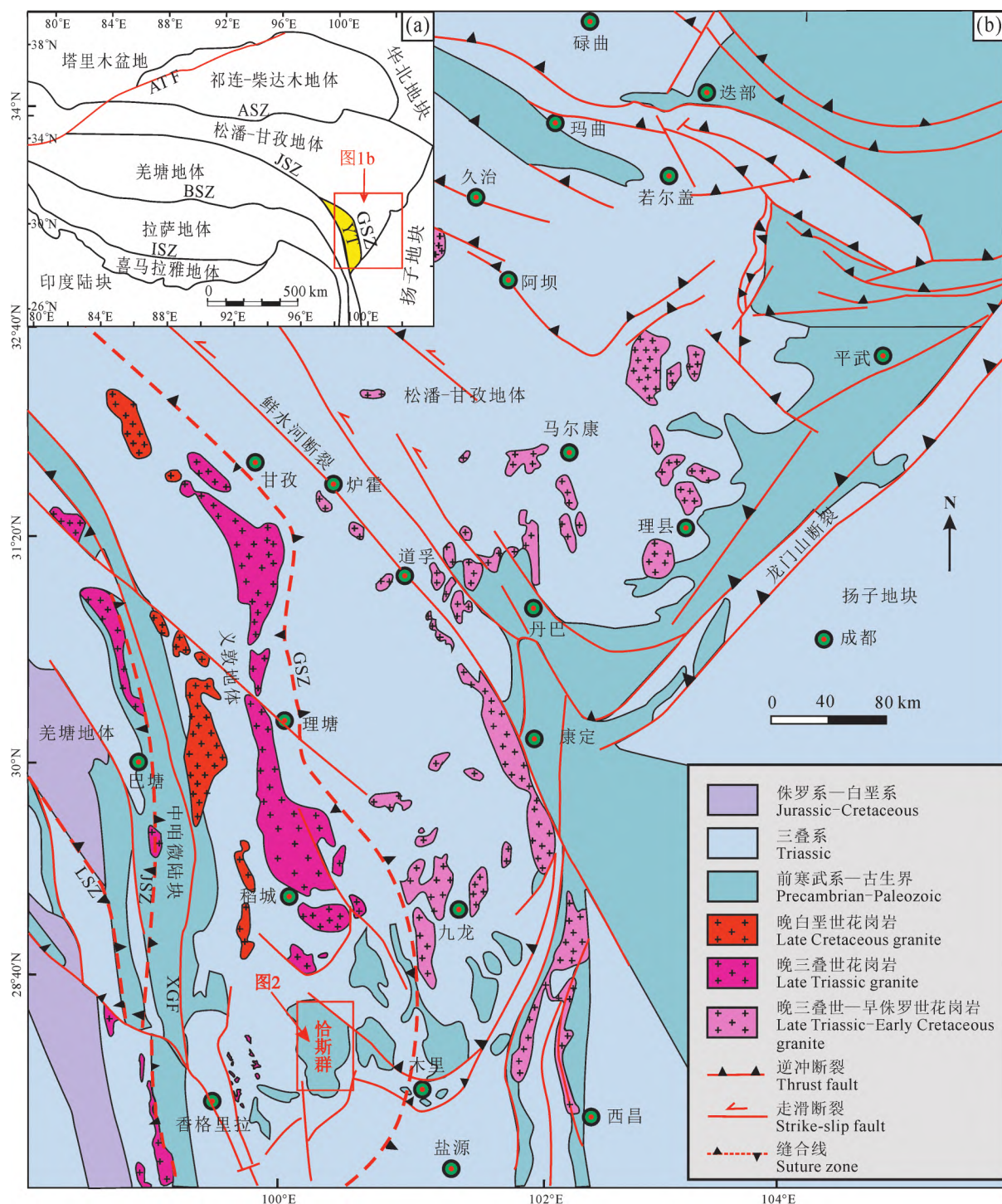


图1 义敦地体及邻区大地构造位置(a)和区域地质简图(b)(据 Tian Zhendong et al., 2020)

Fig 1 Simplified geological map of Yidun Terrane and adjacent region(after Tian Zhendong et al., 2020)

ASZ—阿尼玛卿-勉略缝合带; BSZ—班公-怒江缝合带; GSZ—甘孜-理塘缝合带; ISZ—雅鲁藏布江缝合带; JSZ—金沙江缝合带; LSZ—澜沧江缝合带; ATF—阿尔金断裂; XGF—乡城-格咱断裂; YT—义敦地体

ASZ—A'nyemaqen-Mianlue suture zone; BSZ—Bangong-Nujiang suture zone; GSZ—Ganze-Litang suture zone; ISZ—Indus-Yarlung suture zone; JSZ—Jinshajiang suture zone; LSZ—Lancangjiang suture zone; ATF—Altyn Tagh fault; XGF—Xiangcheng-Geza fault; XSF—Xianshuihe fault; YT—Yidun terrane

西(现今方向)俯冲于义敦地体之下,形成了大量的弧岩浆岩和具有重要经济价值的斑岩-矽卡岩型

Cu-Mo-Au 和 VMS 型 Ag-Pb-Zn 多金属矿床(Hou Zengqian et al., 2001; Li Wenchang et al., 2017;

Leng Chengbiao et al., 2018)。近年来,前人重点对区内大量分布的矿产资源和中生代以来的构造岩浆演化过程进行了研究,而对该地体新元古代—早古生代时期的构造演化过程研究甚少,其构造亲缘性存在较大的争议。由于义敦地体和扬子地块在新元古代—古生代时期具有相似的沉积地层和古生物化石,许多学者认为义敦地体具有亲扬子地块的构造属性(郑裕民等,1984^①; Song Xieyan et al., 2004)。但也有部分专家认为义敦地体并非裂离自扬子地块,而是来自青藏高原东北部的东昆仑地体(Pullen et al., 2008)。Tian Zhendong et al.(2020)对区内成冰纪变沉积岩开展了全岩地球化学及碎屑锆石 U-Pb-Hf 同位素研究,发现义敦地体新元古界变沉积岩碎屑物源主要来自扬子地块西缘同时期的中酸性弧岩浆岩,证实该地体在新元古代具有亲扬子地块的构造属性,两者在新元古代时期可能位于罗迪尼超大陆的边缘。但是,在罗迪尼超大陆裂解(约 750~600 Ma)之后,义敦地体究竟经历了怎样的地质演化过程以及其是否参与了冈瓦纳大陆的形成仍不清楚。

锆石是中酸性岩浆岩、变质岩及碎屑沉积岩中常见的副矿物,记录了地壳主要的岩浆和变质事件(Hoskin and Schaltegger, 2003)。由于其具有极强的抗风化、抗磨蚀和抗蚀变能力,可以在沉积循环过程中保持最初的物源信息,并可以记录那些遭受强烈剥蚀后可能已不存在的岩石信息(Fedo et al., 2003; Gehrels, 2012)。因此,沉积岩中碎屑锆石被广泛应用于示踪沉积物的来源、探讨地体的构造属性、演化过程及古地理重建(Xu Yajun et al., 2013; Wang Wei et al., 2019; Long Xiaoping et al., 2020)。此外,利用沉积岩中最年轻的碎屑锆石 U-Pb 年龄还可以约束地层的最大沉积时限(Gehrels, 2012)。本文对义敦地体恰斯群第四岩性组(形成于早古生代,见下文)三件浅变质沉积岩样品开展了碎屑锆石 U-Pb 年代学和 Hf 同位素研究,并结合已发表文章中新元古界变沉积岩碎屑锆石年龄数据,综合分析其沉积物源随时间的变化情况,探讨义敦地体在新元古代—早古生代时期可能的构造演化过程及其与冈瓦纳大陆的关系。

1 地质背景

义敦地体在大地构造位置上处于羌塘地体、松潘-甘孜地体和扬子地块的结合部位(图 1a)。以近 NNW 走向的乡城-格咱断裂为界,义敦地体可以分

为东、西两个部分。其西部又叫中咱微陆块,主要由古生界的碎屑沉积岩和碳酸盐岩组成(图 1b),另含少量的火山岩夹层;东部主要为上三叠统复理石沉积地层(图 1b),但在其南端恰斯、木里等地出露有前寒武系和古生界的沉积地层(图 2)。

恰斯群是区内目前发现的最古老地层,自下而上可分为四个岩性组。由于有限的地质露头受到严重的坡积物覆盖,恰斯群各岩性组间接触关系尚不明确。第一岩性组主要包括石榴子石钠长片岩、石榴子石云母阳起钠长片岩、二云母石英片岩和浅粒岩,层厚超过 788 m(杜其良, 1986)。第二岩性组厚度约 1050 m,岩性主要为石榴阳起钠长片岩、石榴子石云母石英片岩、绿帘钠长阳起片岩、钠长浅粒岩、钠长二云片岩,另见少量的大理岩、白云质结晶灰岩和长英质火山岩(图 3),LA-ICP-MS 锆石 U-Pb 定年显示火山岩形成时代为 822±4 Ma(田振东, 2020),说明该地层沉积于新元古代,并非前人所认为的古元古代(郑裕民等, 1984^①; 杜其良, 1986)。第三岩性组层厚约 330 m,岩石类型主要为钠长浅粒岩、石英岩、绢云母石英片岩、石榴子石阳起钠长片岩(杜其良, 1986)。他们的原岩主要为沉积岩,形成于成冰纪(约 777~635 Ma)(Tian Zhendong et al., 2020)。碎屑锆石年龄主要集中在 800~780 Ma 和 850~820 Ma,碎屑物源主要来自扬子地块西缘新元古代的中酸性岩浆岩(田振东, 2020)。第四岩性组主要包括钠长片岩、二云母片岩、绿泥石云母片岩、浅粒岩、石英岩,夹少量的大理岩(图 3)。其原岩为长石石英砂岩、粉砂岩、沉凝灰岩和碳酸盐岩(田振东, 2020)。恰斯群第四岩性组在 NE 和 SW 方向分别与埃迪卡拉系和二叠系呈不整合接触(图 2)(杜其良, 1986),其形成时代可能为晚奥陶世—志留纪(详见下文)。由于金沙江古特提斯洋在早三叠世闭合,义敦地体与羌塘地体发生碰撞,恰斯群岩石在该时期经历了绿片岩相的变质作用(田振东等, 2018a, 2018b)。上古生界沉积岩在全区主要为一套滨海相-浅海相的碳酸盐岩沉积,局部含晚二叠世峨眉山玄武岩夹层(图 2)(郑裕民等, 1984^①)。

伴随着甘孜-理塘古特提斯洋的开启、俯冲过程,区内大量发育晚古生代和中生代(集中在晚三叠世和晚白垩世)的岩浆岩(图 1b);前寒武纪和早古生代的岩浆岩在全区均不发育。

2 样品及分析方法

本次研究在恰斯群第四岩性组共采集三件浅

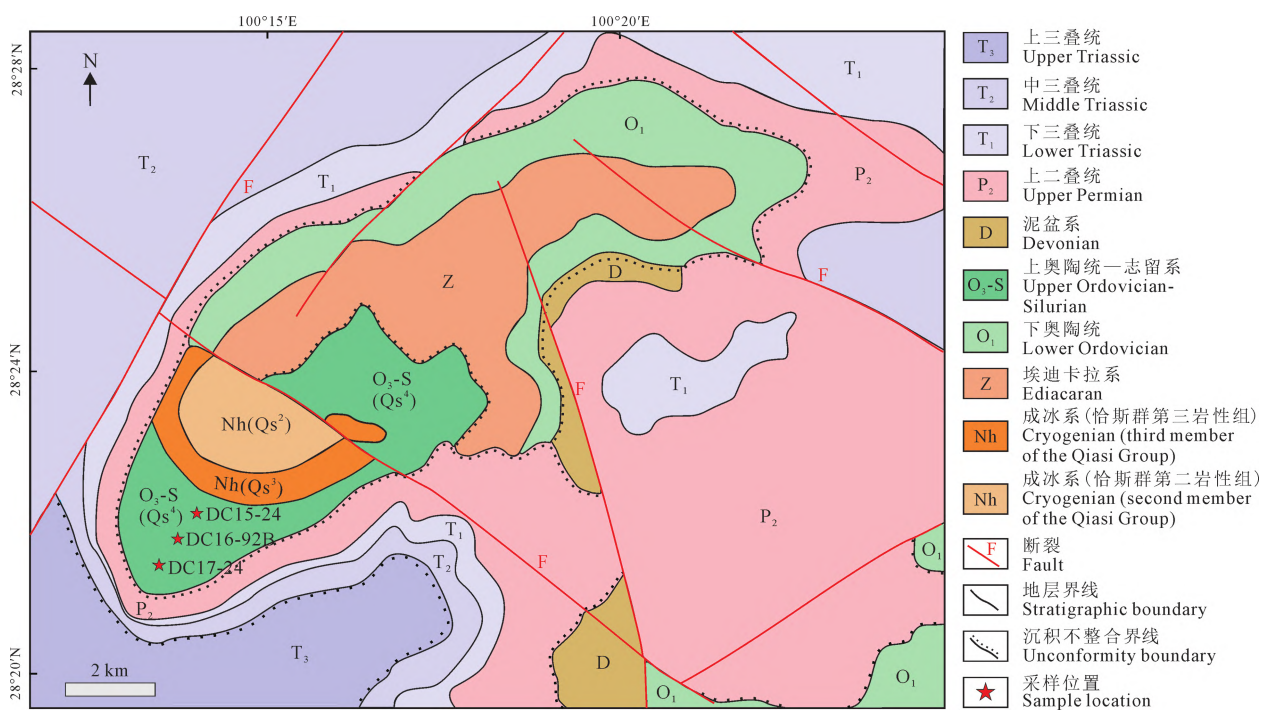


图2 义敦地体恰斯群样品采集区地质简图(据 Tian Zhendong et al., 2020 修改)

Fig. 2 Geological sketch map of the Qiasi Group in the Yidun terrane (modified from Tian Zhendong et al., 2020)

变质沉积岩样品(图2、3)。其中,一件为绿泥石云母片岩(DC16-92B),两件为变长石石英砂岩(DC15-24、DC17-24)。现将其岩石学特征分别描述如下:

绿泥石云母片岩呈墨绿—灰绿色,产出于变长石石英砂岩夹层中(图4a)。其原岩可能为火山—沉积碎屑岩类,含有较多的凝灰质组分。岩石具有鳞片变晶结构,其矿物组成主要包括长石(50%~55%)、石英(15%~20%)、云母(15%~20%)、和绿泥石(5%~10%)(图4c)。岩石中矿物颗粒具有明显的定向性。云母和绿泥石呈鳞片状定向排列(图4c);长石和石英颗粒具有明显的塑性拉长,其长轴方向和云母的排列方向一致。长石颗粒内部多蚀变为黏土矿物。石英颗粒具波状消光现象,次生加大明显。

变长石石英砂岩(图4b)呈灰白色,岩石中石英含量较绿泥石云母片岩明显增多,可达70%~80%;长石含量较低,约占10%~15%。石英颗粒间呈平直或锯齿状紧密镶嵌,具波状消光和次生加大现象(图4d)。长石颗粒发育格子双晶,呈次棱角状(图4d)。此外,该岩石中还含有少量的(约5%~10%)白云母,呈长条状定向分布在石英和长石颗粒间(图4d)。

碎屑锆石的分选工作在宏信地质勘查技术服务

有限公司完成。用传统的重液和磁选方法分离出锆石后,在双目镜下将其粘贴在环氧树脂靶上,并抛光至露出颗粒内部结构。锆石透、反射光、阴极发光图像(CL)和LA-ICP-MS U-Pb定年均在中国科学院地球化学研究所矿床地球化学国家重点实验室完成。其中,CL图像在配备Gatan阴极荧光探头装置的JSM-7088F型扫描电镜上完成;U-Pb定年所使用的激光剥蚀系统为Geolas Pro 193nm ArF准分子激光剥蚀系统,电感耦合等离子体质谱仪型号为Agilent 7900 ICP-MS。激光剥蚀的能量密度为60 mJ,频率为5 Hz,束斑直径为32 μm。分析过程中使用氦气作为载气,每个采集周期包括20 s的空白信号和50 s的样品信号。用标准锆石91500作为外标进行同位素分馏校正,Plešovice和GJ-1作为质量监控。详细的分析测试和离线处理流程见Liu Yongsheng et al. (2008)。碎屑锆石年龄谐和图和概率密度图由Isoplot/Ex_ver 4.15软件绘制完成(Ludwig, 2003)。获得的91500、Plešovice和GJ-1加权平均年龄为1062.3±3.5 Ma (n=40)、337.8±2.2 Ma (n=9)和601.3±5.0 Ma (n=6),与标样的推荐值1062.4±0.8 Ma (Wiedenbeck et al., 1995)、337.13±0.37 Ma (Sláma et al., 2008)和599.8±4.5 Ma (Jackson et al., 2004)在误差范围内一致,证明了测试数据的可靠性。

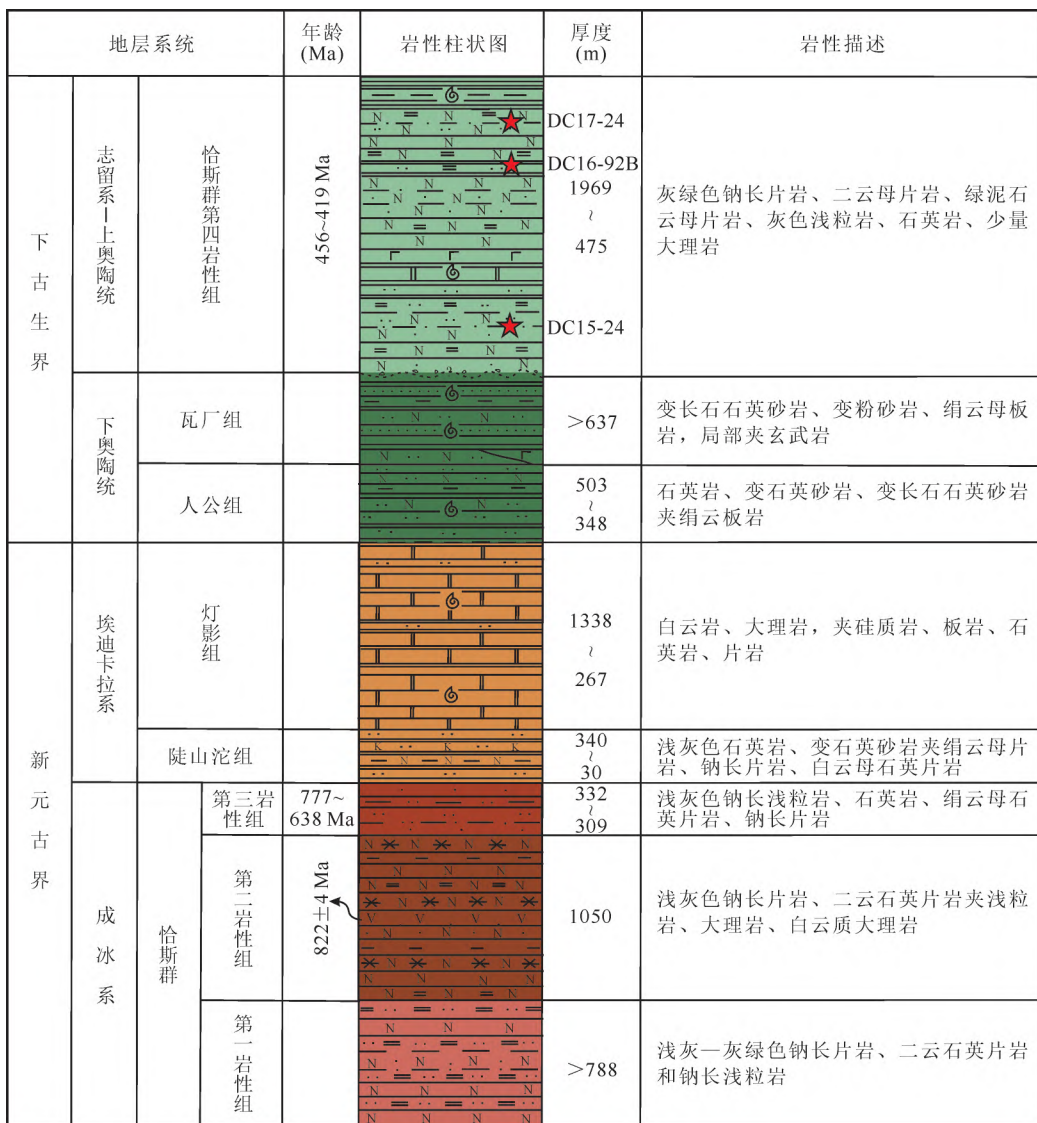
图 3 义敦地体东部新元古界—下古生界地层柱状图(据郑裕民等, 1984^①; 田振东, 2020 修改)

Fig. 3 Stratigraphic column of the Neoproterozoic to lower Paleozoic strata in the eastern Yidun terrane
(modified from Zheng Yumin et al., 1984^①; Tian Zhendong et al., 2020)

锆石 Hf 同位素测试在武汉上谱分析科技有限责任公司完成。分析仪器为配有 Geolas HD 激光取样系统的 Neptune 激光剥蚀-多接受等离子体质谱(LA-MC-ICP-MS), 激光剥蚀的束斑直径为 44 μm , 能量输出密度为 7 J/cm^2 , 频率为 5 Hz。在 $^{176}\text{Hf}/^{177}\text{Hf}$ 测定中, 采用 $^{176}\text{Yb}/^{173}\text{Yb}=0.7963$ 和 $^{176}\text{Lu}/^{176}\text{Lu}=0.02655$ 校正 ^{176}Yb 和 ^{176}Lu 这两个同质异位素对 ^{176}Hf 的影响, 采用 $^{176}\text{Hf}/^{177}\text{Hf}=0.7325$ 校正获得的 $^{176}\text{Hf}/^{177}\text{Hf}$ 比值。样品测试过程中, 标准锆石 91500 和 GJ-1 同时进行了分析, 其获得的 $^{176}\text{Hf}/^{177}\text{Hf}$ 平均值分别为 0.282308 ± 0.000006 和 0.282017 ± 0.000009 , 与标样的推荐值 0.282311 ± 0.000005 (Yuan Honglin et al., 2008) 和 0.282013

± 0.000004 (Yuan Honglin et al., 2008) 误差范围内一致, 表明数据具有高的可靠性。详细的测试条件和操作流程见 Hu Zhaochu et al. (2012), 线下的数据处理过程使用 ICPMSDataCal 软件完成 (Liu Yongsheng et al., 2008)。

在 Hf 同位素初始值计算过程中, ^{176}Lu 的衰变常数采用 $1.865 \times 10^{-11} \text{ a}^{-1}$ (Scherer et al., 2001), 球粒陨石的 $^{176}\text{Lu}/^{177}\text{Hf}=0.0332$, $^{176}\text{Hf}/^{177}\text{Hf}=0.282772$ (Blichert-Toft et al., 1997)。亏损地幔线计算选用现今的 $^{176}\text{Lu}/^{177}\text{Hf}=0.0384$, $^{176}\text{Hf}/^{177}\text{Hf}=0.28325$ (Griffin et al., 2004), 两阶段模式年龄计算过程中采用平均大陆地壳值 $^{176}\text{Lu}/^{177}\text{Hf}=0.015$ (Griffin et al., 2000)。

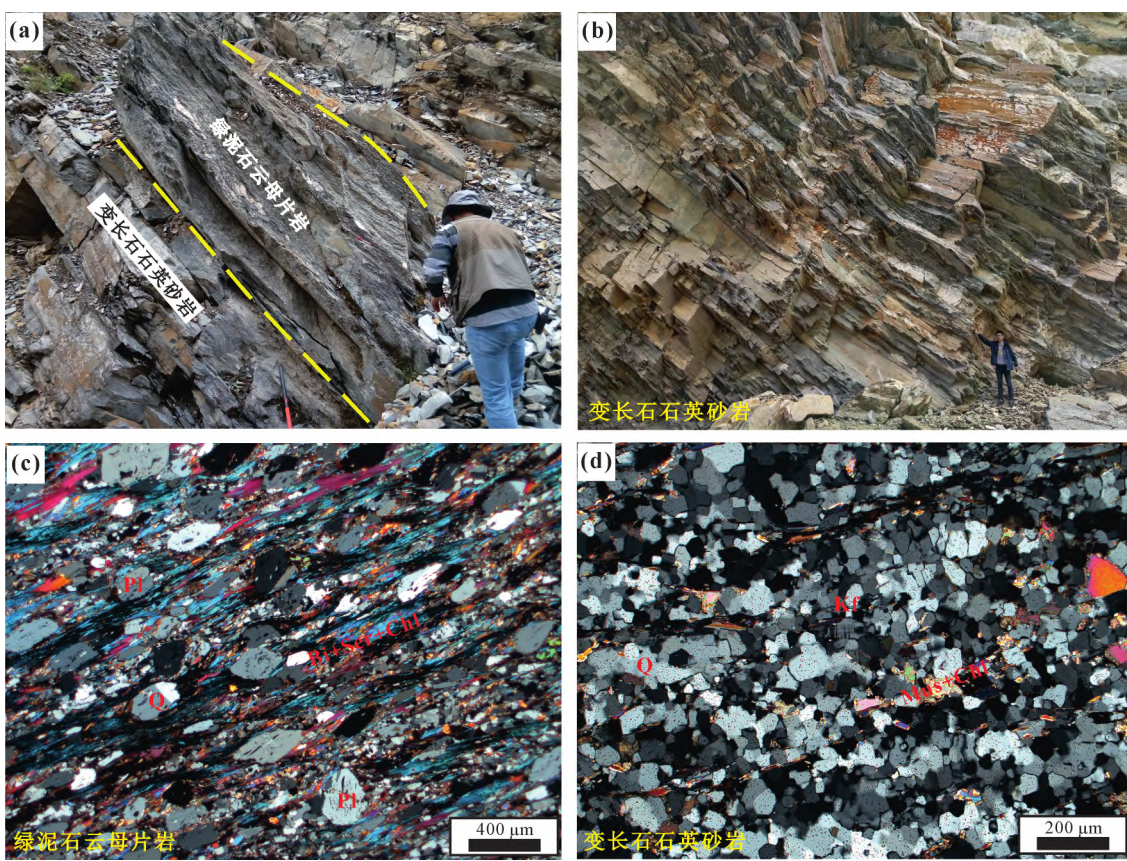


图4 义敦地体恰斯群第四岩性组绿泥石云母片岩、变长石石英砂岩野外露头和镜下特征(正交偏光)

Fig. 4 Photos of field outcrop and microphotographs (orthogonal polarized light) of chlorite-mica schist and meta-feldspathic quartz sandstone from the fourth member of the Qiasi Group, Yidun terrane

3 分析结果

三件样品中代表性碎屑锆石颗粒的CL图像见图5, LA-ICP-MS锆石U-Pb定年结果见附表1和图6, 锆石Hf同位素分析测试结果见附表2和图7。在碎屑锆石年龄频谱图中, 年龄大于1000 Ma采用 $^{207}\text{Pb}/^{206}\text{Pb}$ 年龄, 反之则选用 $^{238}\text{U}/^{206}\text{Pb}$ 年龄。

3.1 锆石形态特征

三件变沉积岩样品中, 锆石颗粒大部分呈无色或淡粉红色, 透明至半透明。颗粒大小不一, 长约60~130 μm , 宽约45~70 μm , 长/宽约1:1至2:1。一部分锆石颗粒具有自形—半自形的长柱状轮廓, 说明其经历了较短距离的搬运过程; 另一部分颗粒则具有一定的磨圆, 呈圆状或次圆状, 反映其经历了一定距离的搬运或沉积物的再循环过程。在CL图像, 这些锆石颗粒绝大多数具有明显或弱的韵律环带, 少数呈现均一的内部结构, 极个别出现核-边结构(图5)。绝大部分锆石具有高的Th/U比值(>0.2, 附表1), 结合其发育典型的岩浆韵律环带, 指

示其为岩浆成因锆石(Hoskin and Schaltegger, 2003); 极个别颗粒具有均一的内部结构和低的Th/U比值(<0.09), 暗示其为变质成因(Hoskin and Schaltegger, 2003)。

3.2 锆石U-Pb年龄

样品DC15-24共分析105个锆石颗粒, 获得了100个有效的(不谐和度小于10%; 下同)年龄数据, 其U-Pb年龄变化范围为 $3114 \pm 35.8 \sim 469 \pm 6.4$ Ma。这些锆石颗粒的年龄主要分布在590~521 Ma($n=17$)、907~739 Ma($n=26$)、1081~932 Ma($n=18$)、2585~2365 Ma($n=15$)四个年龄段(图6), 少数颗粒分布在695~619 Ma($n=6$)和2157~1165 Ma($n=12$)。7颗锆石颗粒具有太古宙的形成年龄, 其 $^{207}\text{Pb}/^{206}\text{Pb}$ 年龄分布在 $3114 \pm 35.8 \sim 2502 \pm 44.9$ Ma之间。

样品DC16-92B从80个测点中共获得76个有效的年龄数据, 其U-Pb年龄变化范围为 $3331 \pm 21.8 \sim 456 \pm 4.7$ Ma。这些锆石颗粒的年龄主要集中在591~519 Ma($n=15$)、888~788 Ma($n=$

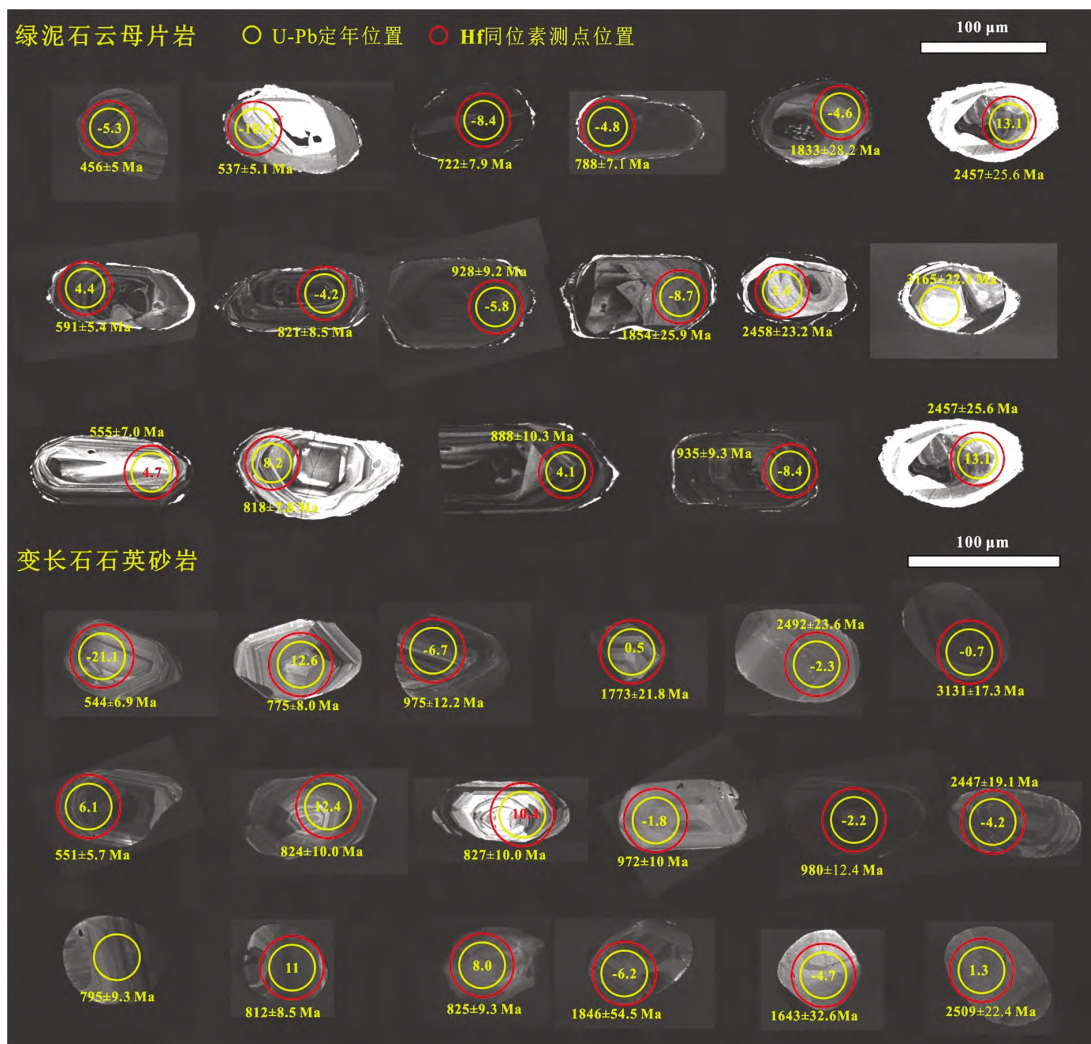


图 5 义敦地体恰斯群第四岩性组代表性碎屑锆石颗粒阴极发光(CL)图像

Fig. 5 Representative CL images of detrital zircons of three samples from the fourth member of the Qiasi Group, Yidun terrane

12)、1094~901 Ma ($n=23$) 和 2469~2351 Ma ($n=6$) 四个年龄段, 它们的测点数分别占分析测试总数的约 20%、16%、30% 和 8%, 对应的峰值年龄分别为 539 Ma、821 Ma、927 Ma 和 2459 Ma (图 6)。少数锆石颗粒年龄分布在 722~616 Ma ($n=5$) 和 2116~1235 Ma ($n=10$) 年龄区间。三颗锆石颗粒具有太古宙的形成年龄, 其 $^{207}\text{Pb}/^{206}\text{Pb}$ 分别为 2794 ± 27.5 Ma、3165 ± 22.1 Ma 和 3331 ± 21.8 Ma。

样品 DC17-24 共分析 95 个锆石颗粒, 获得了 94 个有效的年龄数据, 其 U-Pb 年龄变化范围为 3133~544 Ma。在年龄频谱图上(图 6), 这些锆石颗粒的年龄主要集中在 894~751 Ma ($n=40$, 峰值为 ~825 Ma)、996~956 Ma ($n=14$, 峰值为 ~973 Ma); 其次集中在 2535~2394 Ma ($n=16$, 峰值为 ~2470 Ma) 和 630~544 Ma ($n=5$, 峰值为 ~549

Ma)。7 颗锆石颗粒的 $^{207}\text{Pb}/^{206}\text{Pb}$ 年龄分布在 3131 ± 17.3~2502 ± 24.1 Ma 之间, 反映源区存在太古宙的地壳物质。

3 锆石 Hf 同位素特征

本次分析获得了样品 DC15-24 的 57 颗锆石 Hf 同位素数据, 其 $^{176}\text{Lu}/^{177}\text{Hf}$ 、 $^{176}\text{Hf}/^{177}\text{Hf}$ 、 $\epsilon_{\text{Hf}}(t)$ 和 T_{DM2} 变化范围分别为 0.000019~0.002402、0.280926~0.282575、-22.1~+7.5 和 3533~1124 Ma。其中, 年龄在 590~521 Ma 范围内的锆石颗粒 $^{176}\text{Hf}/^{177}\text{Hf}$ 为 0.281805~0.282502、 $\epsilon_{\text{Hf}}(t)$ 为 -22.1~+2.7, T_{DM2} 为 3118~2114 Ma; 年龄在 907~739 Ma 范围内的锆石颗粒 $^{176}\text{Hf}/^{177}\text{Hf}$ 为 0.281729~0.282454, $\epsilon_{\text{Hf}}(t)$ 为 -20.2~+4.7, T_{DM2} 为 2930~1384 Ma; 年龄在 1081~932 Ma 范围内的锆石颗粒 $^{176}\text{Hf}/^{177}\text{Hf}$ 为 0.281889~0.282302, $\epsilon_{\text{Hf}}(t)$

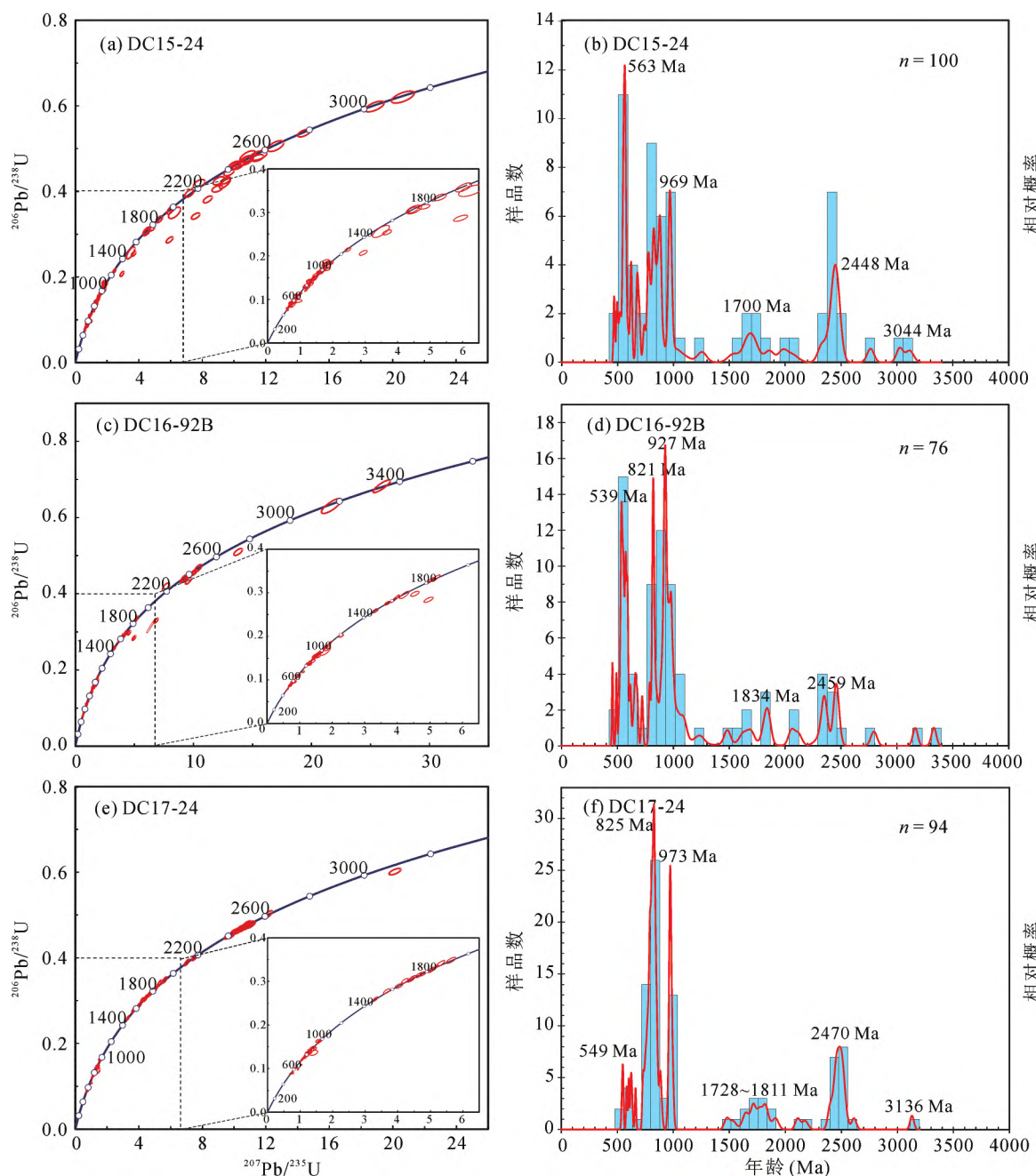


图6 义敦地体恰斯群第四岩性组碎屑锆石U-Pb年龄谱和图(a、c、e)和年龄频谱图(b、d、f)

Fig. 6 U-Pb concordia diagrams (a, c, e) and frequency plots (b, d, f) of detrital zircon from the fourth member of the Qiasi Group, Yidun terrane

为 $-9.4 \sim +6.2$, T_{DM2} 为 $2464 \sim 1517$ Ma; 年龄在 $2585 \sim 2365$ Ma 范围内的锆石颗粒 $^{176}\text{Hf}/^{177}\text{Hf}$ 为 $0.280977 \sim 0.281328$ 、 $\epsilon_{\text{Hf}}(t)$ 为 $-9.5 \sim +5.1$, T_{DM2} 为 $3533 \sim 2735$ Ma (图7)。

样品 DC16-92B 共获得了 58 颗锆石的 Hf 同位素数据, 其 $^{176}\text{Hf}/^{177}\text{Hf}$ 值的变化范围为 $0.280815 \sim 0.282596$ 。其中, 年龄在 $591 \sim 519$ Ma 范围内的锆石颗粒的 $^{176}\text{Hf}/^{177}\text{Hf}$ 值为 $0.281642 \sim 0.282573$ 、

$\epsilon_{\text{Hf}}(t)$ 值为 $-27.6 \sim +4.7$, 两阶段模式年龄(T_{DM2})为 $3228 \sim 1214$ Ma; 年龄在 $888 \sim 788$ Ma 范围内的锆石颗粒的 $^{176}\text{Hf}/^{177}\text{Hf}$ 值为 $0.281912 \sim 0.282537$ 、 $\epsilon_{\text{Hf}}(t)$ 值为 $-12.8 \sim +9.2$, T_{DM2} 为 $2502 \sim 1134$ Ma; 年龄在 $1094 \sim 901$ Ma 范围内的锆石颗粒的 $^{176}\text{Hf}/^{177}\text{Hf}$ 值为 $0.281951 \sim 0.282596$ 、 $\epsilon_{\text{Hf}}(t)$ 值为 $-8.6 \sim +17.1$, T_{DM2} 为 $2330 \sim 829$ Ma; 年龄在 $2469 \sim 2351$ Ma 范围内的锆石颗粒的 $^{176}\text{Hf}/^{177}\text{Hf}$ 值为

0.281215~0.281610, $\epsilon_{\text{Hf}}(t)$ 值为 $-0.7 \sim +13.1$, T_{DM2} 为 $3003 \sim 2161$ Ma (图 7)。

样品 DC17-24 共获得了 60 颗锆石的 Hf 同位素数据, 其 $^{176}\text{Lu}/^{177}\text{Hf}$ 值为 0.000079 ~ 0.007639, $^{176}\text{Hf}/^{177}\text{Hf}$ 值为 0.280805 ~ 0.282694, $\epsilon_{\text{Hf}}(t)$ 值为 $-21.1 \sim +15.7$, T_{DM2} 为 $3551 \sim 883$ Ma。其中, 在 $894 \sim 751$ Ma 年龄段的锆石 $^{176}\text{Hf}/^{177}\text{Hf}$ 值为 $0.281784 \sim 0.282694$, $\epsilon_{\text{Hf}}(t)$ 值为 $-20.1 \sim +12.6$, T_{DM2} 为 $2998 \sim 883$ Ma; 在 $996 \sim 956$ Ma 年龄段的锆石 $^{176}\text{Hf}/^{177}\text{Hf}$ 值为 $0.281914 \sim 0.282451$, $\epsilon_{\text{Hf}}(t)$ 值为 $-11.8 \sim +9.2$, T_{DM2} 为 $2561 \sim 1251$ Ma; 年龄为 $2535 \sim 2394$ Ma 的锆石 $^{176}\text{Hf}/^{177}\text{Hf}$ 值为 $0.280964 \sim 0.281246$, $\epsilon_{\text{Hf}}(t)$ 值为 $-8.8 \sim +1.3$, T_{DM2} 为 $3551 \sim 2926$ Ma。年龄为 $630 \sim 544$

Ma 锆石的 $^{176}\text{Hf}/^{177}\text{Hf}$ 值为 $0.281847 \sim 0.282650$, $\epsilon_{\text{Hf}}(t)$ 值为 $-21.1 \sim +8.9$, T_{DM2} 为 $2813 \sim 1000$ Ma (图 7)。

4 讨论

4.1 恰斯群沉积时限

恰斯群是由四川省地矿局于 1984 年在 1:20 万理塘-稻城-贡岭幅区域地质填图时发现命名 (郑裕民等, 1984^①), 并根据岩石组合、所含的微古植物化石 (如 *Trachysphaereridium* sp.) 和三件全岩样品的 Rb-Sr 等时线年龄 (1972 ± 289 Ma), 将其形成时代置于古元古代 (杜其良, 1986), 但长期缺乏其他同位素年代学数据的佐证。由于 *Trachysphaereridium* sp. 化石分布范围较广, 从

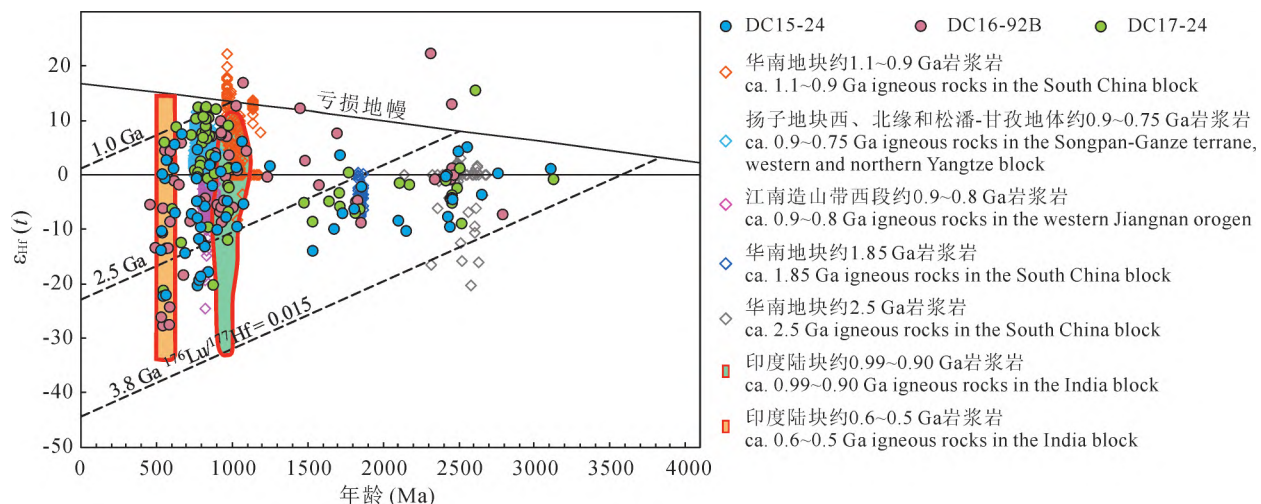


图 7 义敦地体恰斯群第四岩性组碎屑锆石及潜在物源区岩浆锆石 Hf 同位素特征对比图

Fig. 7 Plot of $\epsilon_{\text{Hf}}(t)$ values vs. U-Pb age of detrital zircon from the fourth member of the Qiasi Group, Yidun terrane, and magmatic zircons from the potential sedimentary sources

数据来源: 华南地块约 1.1~0.9 Ga 岩浆岩 (Zhang Aimei et al., 2012; Li Longming et al., 2013; Wang Yuejun et al., 2013, 2014; Chen et al., 2014, 2018; Zhu Weiguang et al., 2016; Li Junyong et al., 2018; Chen Fenglin et al., 2021); 扬子地块西、北缘和松潘-甘孜地体约 0.9~0.75 Ga 岩浆岩 (Huang Xiaolong et al., 2008, 2009; Zhao Junhong et al., 2008, 2010; Zhao Xinfu et al., 2008; Chen Qiong et al., 2015; Meng En et al., 2015; Luo Biji et al., 2018; Zhu Yu et al., 2019a, 2019b); 江南造山带西段约 0.90~0.80 Ga 岩浆岩 (Wang Xiaolei et al., 2006; Zheng Yongfei et al., 2007; Wang Min et al., 2011; Zhao Junhong et al., 2013; Yao Jinlong et al., 2014; Lv Zhengchang et al., 2021); 华南地块约 1.85 Ga 岩浆岩 (Peng Min et al., 2009, 2012; Yu Jinhai et al., 2009); 华南地块约 2.5 Ga 岩浆岩 (Zheng Jianping et al., 2006; Hu Juan et al., 2013); 印度地块约 0.60~0.50 Ga 和约 0.99~0.90 Ga 岩浆岩 $\epsilon_{\text{Hf}}(t)$ 值范围据 Liu Bingbing et al. (2020)

Data sources: ca. 1.1~0.9 Ga igneous rocks in the South China block (Zhang Aimei et al., 2012; Li Longming et al., 2013; Wang Yuejun et al., 2013, 2014; Chen et al., 2014, 2018; Zhu Weiguang et al., 2016; Li Junyong et al., 2018; Chen Fenglin et al., 2021); ca. 0.90~0.75 Ga igneous rocks in the Songpan-Ganze terrane, western and northern Yangtze block (Huang Xiaolong et al., 2008, 2009; Zhao Junhong et al., 2008, 2010; Zhao Xinfu et al., 2008; Chen Qiong et al., 2015; Meng En et al., 2015; Luo Biji et al., 2018; Zhu Yu et al., 2019a, 2019b); ca. 0.90~0.80 Ga igneous rocks in the western Jiangnan orogen (Wang Xiaolei et al., 2006; Zheng Yongfei et al., 2007b; Wang Min et al., 2011; Zhao Junhong et al., 2013; Yao Jinlong et al., 2014; Lv Zhengchang et al., 2021); ca. 1.85 Ga igneous rocks in the South China block (Peng Min et al., 2009, 2012; Yu Jinhai et al., 2009); ca. 2.5 Ga igneous rocks in the South China block (Zheng Jianping et al., 2006; Hu Juan et al., 2013); the fields of ca. 0.99~0.90 Ga igneous rocks from India and Himalaya and ca. 0.60~0.50 Ga igneous rocks from the Pan-African Orogen Belt are modified after Liu Bingbing et al. (2020)

中元古界到下泥盆统中均有分布(龚日祥, 2009), 难以用该化石准确限定恰斯群的沉积时代。Rb-Sr 同位素体系具有低的封闭温度, 极易受到后期热事件的影响, 且仅有三件样品, 因此由四川省地矿局 1984 年报道的等时线年龄具有低的可靠性。田振东(2020)对第二岩性组变火山岩夹层和第三岩性组变沉积岩进行了锆石 U-Pb 定年, 发现变火山岩的形成时代为 822 ± 4 Ma, 第三岩性组变沉积岩的沉积时代为约 $777 \sim 635$ Ma。另外, 恰斯群第四岩性组具有最大的出露面积, 其沉积时代仍未得到精确的同位素年代学限定。

据前人 1:20 万地质填图资料, 恰斯群第四岩性组与区内埃迪卡拉系呈不整合接触(图 2), 前人将该地层划分为前震旦系(杜其良, 1986)。但本次研究发现该层位岩石中有不少锆石颗粒形成于 635 Ma 之后($635 \sim 456$ Ma, $n=25$), 不支持其属于前震旦系。相反, 出现一定数量的早古生代碎屑锆石($541 \sim 456$ Ma, $n=8$)指示其沉积于埃迪卡拉纪之后。本次研究的三件样品中, 最年轻的一粒锆石颗粒年龄为 456 ± 4.7 Ma。由于该锆石颗粒具有高的 Th/U 比值(0.82, 附表 1)、发育岩浆韵律环带(图 5), 反映其未受到后期变质作用或 Pb 丢失的影响, 因此可以代表该地层的最大沉积年龄。鉴于该岩性组所含古生物化石 *Trachysphaereridium* sp. 形成时代不晚于早泥盆世(龚日祥, 2009), 其形成时代应为晚奥陶世—志留纪($456 \sim 419$ Ma)。

综合上述讨论, 我们认为前人将恰斯群定为古元古界是不合适的, 而是应将恰斯群第二至第三岩性组划分为新元古界(成冰系), 第四岩性组定为下古生界(约 $456 \sim 419$ Ma); 由于缺乏可靠的年代学数据, 第一岩性组的沉积时代仍需进一步证实。

4.2 沉积物源分析

如前文所述, 本文研究的恰斯群第四岩性组三件浅变质沉积岩样品具有相似的碎屑锆石年龄谱峰特征和 $\epsilon_{\text{Hf}}(t)$ 值(图 6、7), 反映它们具有相似的物源。因此, 本文不再单独讨论他们的碎屑物源, 而将其合并后进行统一分析。合并后的三件样品中碎屑锆石年龄主要分布在约 $1000 \sim 900$ Ma、约 $890 \sim 750$ Ma 和约 $590 \sim 520$ Ma, 峰值年龄分别为 ~ 973 Ma、 ~ 823 Ma 和 ~ 549 Ma(图 8a); 少量分布在约 $2535 \sim 2350$ Ma 和约 $1900 \sim 1700$ Ma。出现多个不同的年龄峰值指示其源区可能存在多个时代的岩浆岩或来自多个不同的源区。义敦地体除发现有 ~ 822 Ma 变火山岩外(田振东, 2020), 尚无上述其他

年龄段岩浆岩的报道, 说明义敦地体自身并不是恰斯群第四岩性组主要的物源区。由于羌塘地体在晚二叠世—早三叠世才与义敦地体发生拼合(Reid et al., 2005), 因此不可能为区内上奥陶统—志留系沉积岩提供物源。考虑到义敦地体在新元古代—早古生代时期曾是华南地块(包括扬子地块和华夏地块)的一部分, 与松潘—甘孜地体一同位于扬子地块的西缘(Song Xieyan et al., 2004; Tian Zhendong et al., 2020), 因此华南地块和松潘—甘孜地体可能是其潜在的物源区。在前寒武纪时期, 华南地块和松潘—甘孜地体经历了多期次的构造—岩浆事件, 形成了大量的中酸性岩浆岩, 其形成时代可与上述三件样品中前寒武纪多组碎屑锆石年龄相对应(图 9)。

由于义敦地体缺乏新太古代和古元古代的岩浆岩, 约 $2535 \sim 2350$ Ma 和约 $1900 \sim 1700$ Ma 年龄段的碎屑锆石应该来自相邻的地体。前人研究资料表明, 在扬子地块的北部和西南地区出露有约 $2.5 \sim 2.2$ Ga 的岩浆岩, 如约 2.5 Ga 陡岭杂岩(条带状闪长质花岗质片麻岩)(Hu Juan et al., 2013)、鱼洞子地区约 2.5 Ga 钾长花岗岩(Chen Qiong et al., 2019)、 $2.36 \sim 2.22$ Ga 摄科杂岩(二长花岗岩、花岗闪长岩、花岗片麻岩)(Cui Xiaozhuang et al., 2020), 且这些中酸性岩浆岩中的锆石与恰斯群约 $2535 \sim 2350$ Ma 年龄段的碎屑锆石具有相似的 $\epsilon_{\text{Hf}}(t)$ 值和两阶段模式年龄(图 7), 据此我们认为扬子地块约 $2.5 \sim 2.2$ Ga 的岩浆岩可能是义敦地体该年龄段锆石最主要的物源。此外, 在扬子地块的北缘还出露有约 $1.9 \sim 1.8$ Ga 的岩浆岩, 如约 $1.85 \sim 1.82$ Ga 的圈椅端 A 型花岗岩(Xiong Qing et al., 2009; Peng Min et al., 2012)、约 1.85 Ga 华山观环斑花岗岩(Zhang Lijuan et al., 2011)以及侵入崆岭变质基底中的约 1.85 Ga 的基性岩脉(Peng Min et al., 2009), 这些岩浆岩可能是义敦地体 $1700 \sim 1900$ Ma 年龄段碎屑锆石的主要来源。Hf 同位素数据显示, 这一年龄段的碎屑锆石与扬子地块该时期火成岩中岩浆锆石也具有一致的 $\epsilon_{\text{Hf}}(t)$ 值(图 7), 也支持他们源自于这些岩浆岩。此外, 扬子地块西缘古元古界(如大红山群、东川群、河口群)中也含有大量约 $2535 \sim 2350$ Ma 和 $1900 \sim 1700$ Ma 年龄段的碎屑锆石(Greentree et al., 2008; Zhao Xinfu et al., 2010), 这些古老地层的再循环也可能为区内下古生界沉积岩提供了部分物源, 这与部分锆石颗粒具有浑圆状的形态相一致。

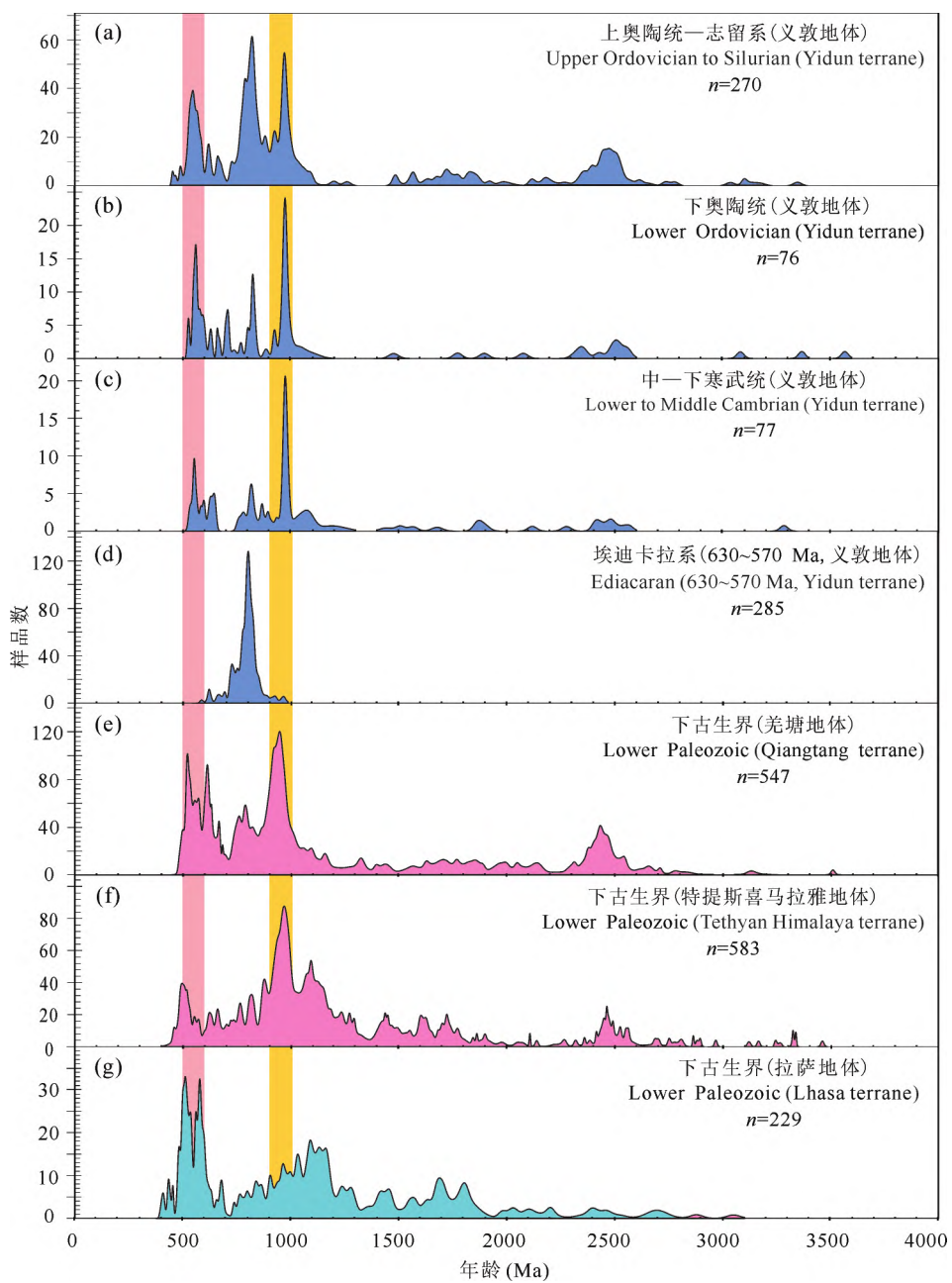


图 8 义敦地体埃迪卡拉纪—志留系沉积岩及羌塘、特提斯喜马拉雅和拉萨地体早古生代沉积岩碎屑锆石年龄谱峰对比图

Fig. 8 U-Pb age probability plots for Ediacaran to Silurian sedimentary rocks in the Yidun terrane and early

Paleozoic sedimentary rocks in the Qiangtang, Tethyan Himalaya, and Lhasa terranes

- (a)—义敦地体上奥陶统一志留系(数据本文);(b)—义敦地体下奥陶统(田振东, 2020);(c)—义敦地体中一下寒武统(田振东, 2020);(d)—义敦地体埃迪卡拉系(Su Bingrui et al., 2020);(e)—羌塘地体下古生界(Pullen et al., 2008; Dong Chunyan et al., 2011; Zhu Dicheng et al., 2011);(f)—特提斯喜马拉雅地体下古生界(Myrow et al., 2009, 2010; Hughes et al., 2011; McQuarrie et al., 2013);(g)—拉萨地体(Zhang Hongfei et al., 2008; Dong Xin et al., 2010)
- (a)—Upper Ordovician to Silurian in the Yidun terrane (this study); (b)—Lower Ordovician in the Yidun terrane (Tian Zhendong, 2020); (c)—Lower to Middle Cambrian in the Yidun terrane (Tian Zhendong, 2020); (d)—Ediacaran in the Yidun terrane (Su Bingrui et al., 2020); (e)—Lower Paleozoic in the Qiangtang terrane (Pullen et al., 2008; Dong Chunyan et al., 2011; Zhu Dicheng et al., 2011); (f)—Lower Paleozoic in the Tethyan Himalaya terrane (Myrow et al., 2009, 2010; Hughes et al., 2011; McQuarrie et al., 2013); (g)—Lower Paleozoic in the Lhasa terrane (Zhang Hongfei et al., 2008; Dong Xin et al., 2009, 2010)

新元古代时期,扬子地块的西缘和北缘经历了俯冲相关的岩浆活动,形成了大量的中酸性弧岩浆

岩(约 870~730 Ma),如康定片麻状花岗岩(797~795 Ma; Zhou Meifu et al., 2002)、石棉花岗岩(790

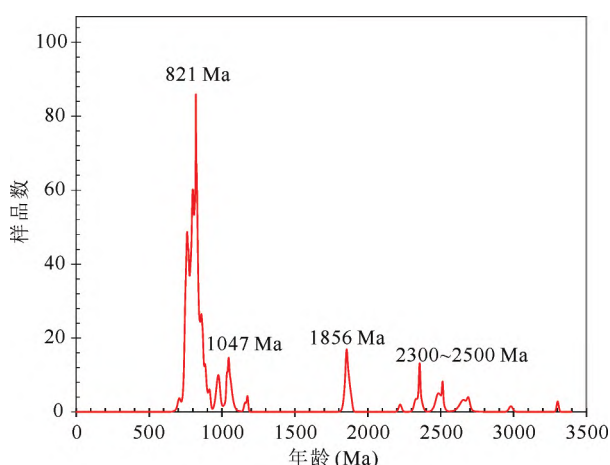


图 9 松潘-甘孜地体和华南地块前寒武纪岩浆岩年龄分布图

Fig. 9 Age distribution of Precambrian igneous rocks in the Songpan-Ganze terrane and South China block

数据引自(data are from): Peng Min et al., 2009, 2012; Xiong Qing et al., 2009; Yu Jinhai et al., 2009; Gao shan et al., 2011; Hu Juan et al., 2013; Li Longming et al., 2013; Wang Yuejun et al., 2013, 2014; Chen et al., 2014, 2018; Wang Xiaolei et al., 2014; Zhou Guangyan et al., 2018; Zhao Junhong et al., 2018; Chen Qiong et al., 2019; Cui Xiaozhuang et al., 2020; Lv Zhenghang et al., 2021

~786 Ma; Zhao Xinfu et al., 2008)、冕宁花岗岩(780~767 Ma; Huang Xiaolong et al., 2008)、茨达花岗岩(~835 Ma; Zhu Yu et al., 2019a)、雪龙包杂岩(~748 Ma; Zhou Meifu et al., 2006)、西乡闪长岩(~764 Ma; Zhao Junhong et al., 2010)等。这些岩浆岩可能为义敦地体上奥陶统一志留系(456~419 Ma)的沉积地层提供了部分碎屑物质,这一推测与两者具有相似的 Hf 同位素组成相一致(图 7)。在图 5 中,约 890~750 Ma 年龄段的碎屑锆石部分颗粒呈浑圆状,反映他们经历了较长距离的搬运或沉积再循环过程。这些浑圆状的锆石不可能来自邻近的松潘-甘孜地体和扬子地块同时期岩浆岩,而应来自别的物源区。前人研究表明,在华南地块江南造山带的西段也同样发育有新元古代的岩浆岩,如元宝山花岗岩(827±7 Ma; Zhao Junhong et al., 2013)、峒马花岗岩(824±13 Ma; Wang Xiaolei et al., 2006)、三防花岗岩(834±8 Ma; Zhao Junhong et al., 2013)、梵净山花岗岩(~830 Ma; Lv Zhenghang et al., 2021)、本洞花岗岩(811±9 Ma; Zhao Junhong et al., 2013)、田朋花岗岩(794±8 Ma; Wang Xiaolei et al., 2006)。这些花岗岩多具有负的 $\epsilon_{\text{Hf}}(t)$ 值(图 7),与约 890~750 Ma 年龄段浑圆状锆石颗粒 Hf 同位素组成相似(图 7),反映这

些岩浆岩可能为该年龄段碎屑锆石的沉积物源。

1000~900 Ma 年龄段碎屑锆石是恰斯群第四岩性组变沉积岩中重要的组成部分,约占总分析颗粒数的 20%。考虑到义敦地体和松潘-甘孜地体并不发育该年龄段的岩浆岩,基本排除了来自这两个地体的可能性。虽然邻区华南地块报道有 1000~900 Ma 岩浆岩(Zhang Aimei et al., 2012; Li Longming et al., 2013; Chen et al., 2014; Li Junyong et al., 2018),但这些岩石主要为基性岩、规模较小,且其锆石多具有正的 $\epsilon_{\text{Hf}}(t)$ 值(图 7),与我们样品中该年龄段碎屑锆石出现大量负的 $\epsilon_{\text{Hf}}(t)$ 值不相符,也排除了这些岩浆岩为其提供大量碎屑物源的可能。此外,部分 1000~900 Ma 年龄段的碎屑锆石具有自形一半自形的轮廓(图 5),也不支持它们来自区域老地层的再循环。除少量的火山岩夹层外,义敦地体和邻区松潘-甘孜地体、扬子地块也同样不发育新元古代晚期—早古生代的岩浆岩,排除了这些地体(块)为 590~520 Ma 年龄段碎屑锆石提供物源的可能。虽然华夏地块出露有早古生代的岩浆岩(Zhao Kuidong et al., 2013),但其形成时代(约 460~400 Ma)明显晚于这类碎屑锆石的结晶年龄(520~590 Ma),说明华夏地块也不是其主要的沉积物源。扬子地块、松潘-甘孜地体和义敦地体寒武纪—奥陶纪沉积岩中含有约 590~520 Ma 年龄段的碎屑锆石(Chen Qiong et al., 2021; Zhou Xueyao et al., 2018),但我们研究的样品中很多约 590~520 Ma 锆石颗粒具有自形一半自形的形态,而不具有再循环成因的次圆或圆状特征,说明其并非区内寒武系—奥陶系沉积岩再循环的产物。因此,我们推测某一地块在早古生代可能与义敦地体相连,为后者提供 1000~900 Ma 和 590~520 Ma 的碎屑物质,但在后期的地质演化过程与义敦地体分离。前人研究表明:东冈瓦纳大陆包含有大量 1000~900 Ma 和 590~520 Ma 的岩浆岩,它们主要分布在 Rayner-Eastern Ghats 造山带(990~900 Ma)、Prydz-Darling 造山带(600~500 Ma)和 Kuunga 造山带(600~500 Ma)(Boger et al., 2001; Jung et al., 2001; Mikhalsky et al., 2011; Morrissey et al., 2015; Goscombe et al., 2020),这些岩石可能是义敦地体下古生界变沉积岩中 1000~900 Ma 和 590~520 Ma 年龄段碎屑锆石的主要物源。Hf 同位素证据显示,这两个年龄段的碎屑锆石与东冈瓦纳大陆同时期岩浆岩中岩浆锆石具有十分相似的 $\epsilon_{\text{Hf}}(t)$ 值和两阶段模式年龄(图 7),

支持其源自这些岩浆岩。

4.3 对区域构造演化的启示

Tian Zhendong et al. (2020)对恰斯群成冰系(恰斯群第三岩性组)变沉积岩进行了研究,发现其碎屑物源主要来自邻区扬子地块和松潘-甘孜地体新元古代的弧岩浆岩,并提出义敦地体在成冰纪可能和扬子地块一同处于罗迪尼超大陆的边缘位置。古地理重建显示,罗迪尼超大陆在新元古代晚期发生裂解之后,华南地块(包括扬子地块和华夏地块)成为了原特提斯洋中一个孤立的块体(Zhao Guochun et al., 2018; Chen Qiong et al., 2021)。由于义敦地体曾是扬子地块的一部分,直至晚古生代甘孜-理塘古特提斯洋打开才与扬子地块分离,因此在新元古代晚期应和扬子地块一同处于原特提斯洋中。在这期间,大洋阻隔了他们与周围其他地块的相互物质交换,其碎屑物源应来自它们内部的隆起区。Su Bingrui et al. (2020)对义敦地体埃迪卡拉系下部的变沉积岩(如石鼓群,沉积于约 630~570 Ma)进行了研究,认为石鼓群的沉积物源主要来自相邻的华南地块,支持义敦地体在埃迪卡拉纪早期可能仍处于原特提斯洋这一古地理格局。

本次研究显示,义敦地体恰斯群第四岩性组三件上奥陶统—志留系浅变质沉积岩中含有大量来自

印度地块 Rayner-Eastern Ghats、Prydz-Darling 或 Kuunga 造山带的碎屑物质,这与区内埃迪卡拉纪早期形成的沉积岩物源主要来自邻区华南地块明显不同,暗示其古地理格局在埃迪卡拉纪晚期—早古生代发生了明显的改变。邻区扬子地块下古生界沉积岩也同样记录了这一现象(Duan Liang et al., 2011; Xu Yajun et al., 2013; Chen Qiong et al., 2021),暗示义敦地体和扬子地块在埃迪卡拉纪晚期或早寒武世与印度地块发生拼合,并接受来自东冈瓦纳大陆的碎屑物质。由于义敦地体和扬子地块缺乏相关的岩浆或变质记录,其发生碰撞的时间难以准确限定。考虑到义敦地体埃迪卡拉纪下部的变沉积岩(如石鼓群,635~570 Ma)碎屑物源与成冰系变沉积岩相似,仍主要源自邻区华南地块(Su Bingrui et al., 2020; Tian Zhendong et al., 2020);而下一中寒武统变沉积岩已出现大量来自印度地块来源的碎屑物质(田振东,2020),据此我们推测义敦地体可能在 570~520 Ma 期间与印度地块发生拼合(图 10),成为了冈瓦纳大陆的一部分。由图 8 可知,区内寒武系—志留系变沉积岩具有相似的碎屑锆石年龄谱峰,反映义敦地体在早古生代时期处于一个稳定的大地构造环境,持续接受来自冈瓦纳大陆的碎屑物质。据此我们推测,义敦地体可能与冈

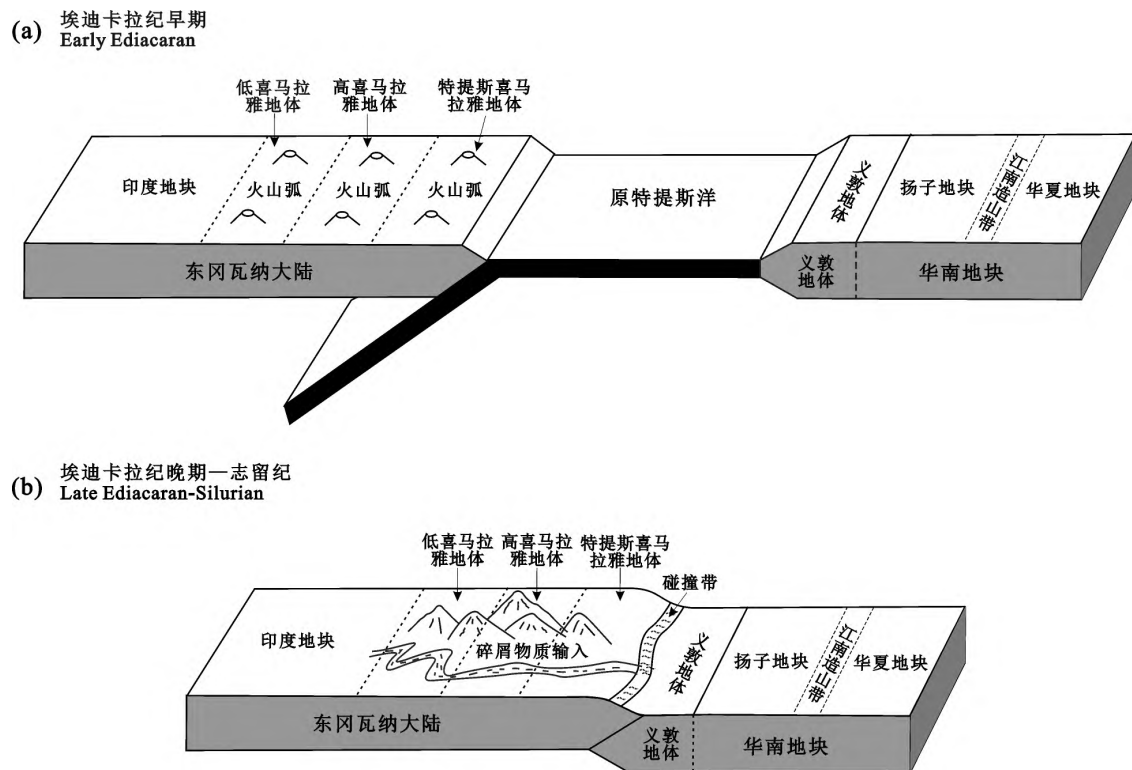


图 10 义敦地体埃迪卡拉纪—早古生代构造演化模型

Fig. 10 Tectonic evolution model of Yidun terrane in the Ediacaran to early Paleozoic periods

瓦纳大陆保持联系直至志留纪(图10)。在早泥盆世,由于金沙江古特提斯洋的打开(Metcalfe I., 2021),义敦地体可能才从东冈瓦纳大陆裂离出来,并向北逐渐漂移至欧亚大陆的边缘。碎屑锆石年龄谱峰对比进一步显示,义敦地体下古生界变沉积岩样品与羌塘和特提斯喜马拉雅地体具有相似的谱峰特征,而缺乏拉萨地体特征的年龄峰(~ 1170 Ma)(图8),说明义敦地体在早古生代时期可能位于东冈瓦纳大陆的北缘,邻近羌塘和特提斯喜马拉雅地体(图10)。

5 结论

(1) 藏东义敦地体恰斯群第四岩性组并非形成于古元古代,而是沉积于晚奥陶世—志留纪(456~419 Ma)。

(2) 义敦地体早古生代沉积岩碎屑物源除来自邻区松潘-甘孜地体和华南地块外,还有大量印度地块来源物质的供给。

(3) 义敦地体在早古生代时期位于冈瓦纳大陆的北缘,邻近羌塘和特提斯喜马拉雅地体,直至志留纪之后才与东冈瓦纳大陆分离。

致谢:本文在修改过程中得到了两位匿名审稿专家非常详尽的修改意见和建议,实验过程中得到了中国科学院地球化学研究所唐燕文老师和武汉上谱分析科技有限责任公司陈红芳老师的帮助,在此一并表示感谢。

附件:本文附件(附表1、2)详见 http://www.geojournals.cn/dzxb/dzxb/article/abstract/202304094?st=article_issue。

注 释

① 郑裕民,王忠实,杜其良,廖远安,李世林. 1984. 1:20万理塘幅、稻城幅、贡岭幅区域地质调查报告.

References

- Blichert-Toft J, Albarede F. 1997. The Lu-Hf geochemistry of chondrites and evolution of chondrites and evolution of the mantle-crust system. *Earth and Planetary Science Letters*, 148 (1-2): 243~258.
- Boger S D, Wilson C J L, Fanning C M. 2001. Early Paleozoic tectonism within the East Antarctic craton: The final suture between east and west Gondwana? *Geology*, 29(5): 463~466.
- Chen Fenglin, Cui Xiaozhuang, Lin Shoufa, Wang Jian, Yang Xueming, Ren Guangming, Pang Weihua. 2021. The 1.14 Ga mafic intrusions in the SW Yangtze Block, South China: Records of late Mesoproterozoic intraplate magmatism. *Journal of Asian Earth Sciences*, 205: 104603.
- Chen Qiong, Sun Min, Long Xiaoping, Yuan Chao. 2015. Petrogenesis of Neoproterozoic adakitic tonalites and high-K granites in the eastern Songpan-Ganze fold belt and implications for the tectonic evolution of the western Yangtze Block. *Precambrian Research*, 270: 181~203.
- Chen Qiong, Sun Min, Zhao Guochun, Zhao Junhong, Zhu Weilin, Long Xiaoping, Wang Jun. 2019. Episodic crustal growth and reworking of the Yudongzi terrane, South China: Constraints from the Archean TTGs and potassic granites and Paleoproterozoic amphibolites. *Lithos*, 326-327: 1~18.
- Chen Qiong, Zhao Guochun, Sun Min. 2021. Protracted northward drifting of South China during the assembly of Gondwana: Constraints from the spatial-temporal provenance comparison of Neoproterozoic-Cambrian strata. *Geological Society of America Bulletin*, 133(9-10): 1947~1963.
- Chen Wei Terry, Sun Weihua, Wang Wei, Zhao Junhong, Zhou Meifu. 2014. "Grenvillian" intra-plate mafic magmatism in the southwestern Yangtze Block, SW China. *Precambrian Research*, 242: 138~153.
- Chen W T, Sun Weihua, Zhou Meifu, Wang Wei. 2018. Ca. 1050 Ma intra-continental rift-related A-type felsic rocks in the southwestern Yangtze Block, South China. *Precambrian Research*, 309: 22~44.
- Cui Xiaozhuang, Wang Jian, Ren Guangming, Deng Qi, Sun Zhiming, Ren Fei, Chen Fenglin. 2020. Paleoproterozoic tectonic evolution of the Yangtze Block: New evidence from ca. 2.36 to 2.22 Ga magmatism and 1.96 Ga metamorphism in the Cuoke complex, SW China. *Precambrian Research*, 337: 105525.
- Dong Chunyan, Li Cai, Wan Yusheng, Wang Wei, Wu Yanwang, Xie Hangqiang, Liu Dunyi. 2011. Detrital zircon age mode of Ordovician Wenquan quartzite south of Lungmuco-Shuanghu suture in the Qiangtang area, Tibet; Constraint on tectonic affinity and source regions. *Science China Earth Sciences*, 54 (7): 1034~1042.
- Dong Xin, Zhang Zeming, Wang Jinlin, Zhao Guochun, Liu Feng, Wang Wei, Yu Fei. 2009. Provenance and formation age of the Nyingchi Group in the southern Lhasa Terrane, Tibetan Plateau: Petrology and zircon U-Pb geochronology. *Acta Petrologica Sinica*, 25 (7): 1678~1694 (in Chinese with English abstract).
- Dong Xin, Zhang Zeming, Santosh M. 2010. Zircon U-Pb chronology of the Nyingtri Group, southern Lhasa Terrane, Tibetan Plateau: Implications for Grenvillian and Pan-African provenance and Mesozoic-Cenozoic metamorphism. *The Journal of Geology*, 118(6): 677~690.
- Du Qiliang. 1986. The discovery and subdivision of Precambrian in Shuiluo area, Muli Country, Sichuan Province. *Journal of Chengdu College of Geology*, 13(1): 31~49 (in Chinese with English abstract).
- Duan Liang, Meng Qingren, Zhang Chengli, Liu Xiaoming. 2011. Tracing the position of the South China block in Gondwana: U-Pb ages and Hf isotopes of Devonian detrital zircons. *Gondwana Research*, 19(1): 141~149.
- Fedo C M, Sircombe K N, Rainbird R H. 2003. Detrital zircon analysis of the sedimentary record. *Reviews in Mineralogy and Geochemistry*, 53(1): 277~303.
- Gao Shan, Yang Jie, Zhou Lian, Li Ming, Hu Zhaochu, Guo Jingliang, Yuan Honglin, Gong Hujun, Xiao Gaoqiang, Wei Junqi. 2011. Age and growth of the Archean Kongling terrane, South China, with emphasis on 3.3 Ga granitoid gneisses. *American Journal of Science*, 311: 153~182.
- Gehrels G. 2012. Detritalzircon U-Pb geochronology: Current methods and new opportunities. In: Azor C B A, ed. *Tectonics of Sedimentary Basins: Recent Advances*. Blackwell Publishing Ltd, Oxford, 45~62.
- Gong Rixiang, Yan Tiezeng, Yu Xinqi, Hua Xihong, Zhang Zhifang. 2009. Subdivision and geological age of Pingshui Group in Zhejiang, China. *Geoscience*, 23(2): 238~245 (in Chinese with English abstract).
- Goscombe B, Foster D A, Gray D, Wade B. 2020. Assembly of central Gondwana along the Zambezibelt: Metamorphic response and basement reactivation during the Kuunga

- Orogeny. *Gondwana Research*, 80: 410~465.
- Greentree M R, Li Zhengxiang. 2008. The oldest known rocks in south-western China: SHRIMP U-Pb magmatic crystallisation age and detrital provenance analysis of the Paleoproterozoic Dahongshan Group. *Journal of Asian Earth Sciences*, 33(5-6): 289~302.
- Griffin W L, Pearson N J, Belousova E, Jackson S E, van A E, O'Reilly S Y, Shee S R. 2000. The Hf isotope composition of cratonic mantle: LAM-MC-ICPMS analysis of zircon megacrysts in kimberlites. *Geochimica et Cosmochimica Acta*, 64(1): 133~147.
- Griffin W L, Belousova E A, Shee S R, Pearson N J, O'Reilly S Y. 2004. Archean crustal evolution in the northern Yilgarn Craton: U-Pb and Hf-isotope evidence from detrital zircons. *Precambrian Research*, 131(3-4): 231~282.
- Grocholski Brent. 2019. Ancient height of the Tibetan Plateau. *Science*, 363: 911~943.
- Hoskin P W O, Schaltegger U. 2003. The composition of zircon and igneous and metamorphic petrogenesis. 53: 25~104.
- Hou Zengqian, Khin Zaw, Qu Xiaoming, Ye Qingtong, Yu Jinjie, Xu Mingji, Fu Deming, Xianke Yin. 2001. Origin of the Gacun volcanic-hosted massive sulfide deposit in Sichuan, China: Fluid inclusion and oxygen isotope evidence. *Economic Geology*, 96 (7): 1491~1512.
- Hu Juan, Liu Xiaochun, Chen Longyao, Qu Wei, Li Huakun, Geng Jianzhen. 2013. A ~ 2.5 Ga magmatic event at the northern margin of the Yangtze craton: Evidence from U-Pb dating and Hf isotope analysis of zircons from the Douling complex in the South Qinling orogen. *Chinese Science Bulletin*, 58(28-29): 3564~3579.
- Hu Peiyuan, Zhai Qingguo, Zhao Guochun, Wang Jun, Tang Yue, Zhu Zhicai, Wu Hao. 2019. The North Lhasa terrane in Tibet was attached with the Gondwana before it was drafted away in Jurassic: Evidence from detrital zircon studies. *Journal of Asian Earth Sciences*, 185: 104055.
- Hu Zhaochu, Liu Yongsheng, Gao Shan, Liu Wengui, Zhang Wen, Tong Xirun, Lin Lin, Zong Keping, Li Ming, Chen Haihong, Zhou Lian, Yang Lu. 2012. Improved in situ Hf isotope ratio analysis of zircon using newly designed X skimmer cone and jet sample cone in combination with the addition of nitrogen by laser ablation multiple collector ICP-MS. *Journal of Analytical Atomic Spectrometry*, 27(9): 1391~1399.
- Huang Xiaolong, Xu Yigang, Li Xianhua, Li Wuxian, Lan Jiangbo, Zhang Huihuang, Liu Yongsheng, Wang Yanbin, Li Hongyan, Luo Zhengyu, Yang Qijun. 2008. Petrogenesis and tectonic implications of Neoproterozoic, highly fractionated A-type granites from Mianning, South China. *Precambrian Research*, 165(3): 190~204.
- Huang Xiaolong, Xu Yigang, Lan Jiangbo, Yang Qijun, Luo Zhengyu. 2009. Neoproterozoic adakitic rocks from Mopanshan in the western Yangtze Craton: Partial melts of a thickened lower crust. *Lithos*, 112(3): 367~381.
- Hughes N C, Myrow P M, McKenzie N, Harper D A T, Bhargava O N, Tangri S K, Ghaleey K S, Fanning C M. 2011. Cambrian rocks and faunas of the Wachia La, Black Mountains, Bhutan. *Geological Magazine*, 148(3): 351~379.
- Jackson S E, Pearson N J, Griffin W L, Belousova E A. 2004. The application of laser ablation-Inductively coupled plasma-mass spectrometry to in situ U-Pb zircon geochronology. *Chemical Geology*, 211: 47~69.
- Jung S, Mezger K, Hoernes S. 2001. Trace element and isotopic (Sr , Nd , Pb , O) arguments for a mid-crustal origin of Pan-African garnet-bearing S-type granites from the Damara orogen (Namibia). *Precambrian Research*, 110(1): 325~355.
- Leng Chengbiao, Gao Jianfeng, Chen W T, Zhang Xingchuan, Tian Zhendong, Guo Jianheng. 2018. Platinum-group elements, zircon Hf-O isotopes, and mineralogical constraints on magmatic evolution of the Pulang porphyry Cu-Au system, SW China. *Gondwana Research*, 62: 163~177.
- Li Junyong, Wang Xiaolei, Gu Zhidong. 2018. Early Neoproterozoic arc magmatism of the Tongmuliang Group on the northwestern margin of the Yangtze Block: Implications for Rodinia assembly. *Precambrian Research*, 309: 181~197.
- Li Longming, Lin Shoufa, Xing Guangfu, Davis D W, Davis W J, Xiao Wenjiao, Yin Changqing. 2013. Geochemistry and tectonic implications of late Mesoproterozoic alkaline bimodal volcanic rocks from the Tieshajie Group in the southeastern Yangtze Block, South China. *Precambrian Research*, 230: 179~192.
- Li Wenchang, Yu Hajun, Gao Xue, Liu Xuelong, Wang Jianhua. 2017. Review of Mesozoic multiple magmatism and porphyry Cu-Mo (W) mineralization in the Yidun arc, eastern Tibet Plateau. *Ore Geology Reviews*, 90: 795~812.
- Li Bingbing, Peng Touping, Fan Weiming, Zhao Guochun, Gao Jianfeng, Dong Xiaohan, Peng Bingxia. 2020. Tectonic evolution and paleoposition of the Baoshan and Lincang blocks of west Yunnan during the Paleozoic. *Tectonics*, 39(10).
- Liu Yongsheng, Hu Zhaochu, Gao Shan, Günther Detlef, Xu Juan, Gao Changgui, Chen Haihong. 2008. In situ analysis of major and trace elements of anhydrous minerals by LA-ICP-MS without applying an internal standard. *Chemical Geology*, 257 (1-2): 34~43.
- Long Xiaoping, Luo Jin, Sun Min, Wang Xuance, Wang Yujing, Yuan Chao, Jiang Yingde. 2020. Detrital zircon U-Pb ages and whole-rock geochemistry of early Paleozoic metasedimentary rocks in the Mongolian Altai: Insights into the tectonic affinity of the whole Altai-Mongolian terrane. *Geological Society of America Bulletin*, 132(3-4): 477~494.
- Ludwig K R. 2003. ISOPLOT 3.00: A geochronological toolkit for Microsoft Excel. Berkeley Geochronology Center, Berkeley, California, 4, 1~71.
- Luo Biji, Liu Rong, Zhang Hongfei, Zhao Junhong, Yang He, Xu Wangchun, Guo Liang, Zhang Liqi, Tao Lu, Pan Fabin, Wang Wei, Gao Zhong, Shao Hui. 2018. Neoproterozoic continental back-arc rift development in the northwestern Yangtze Block: Evidence from the Hannan intrusive magmatism. *Gondwana Research*, 59: 27~42.
- Lv Zhenghang, Chen Juan, Zhang Hui, Tang Yong. 2021. Petrogenesis of Neoproterozoic rare metal granite-pegmatite suite in Jiangnan orogen and its implications for rare metal mineralization of peraluminous rock in South China. *Ore Geology Reviews*, 128: 103923.
- Ma Anlin, Hu Xiumian, Garzanti E, Han Zhong, Lai Wen. 2017. Sedimentary and tectonic evolution of the southern Qiangtang basin: Implications for the Lhasa-Qiangtang collision timing. *Journal of Geophysical Research: Solid Earth*, 122 (7): 4790~4813.
- McQuarrie N, Long S P, Tobgay T, Nesbit J N, Gehrels G, Ducea M N. 2013. Documenting basin scale, geometry and provenance through detrital geochemical data: Lessons from the Neoproterozoic to Ordovician Lesser, Greater, and Tethyan Himalayan strata of Bhutan. *Gondwana Research*, 23 (4): 1491~1510.
- Meng En, Liu Fulai, Du Lilin, Liu Pinghua, Liu Jianhui. 2015. Petrogenesis and tectonic significance of the Baoxing granitic and mafic intrusions, southwestern China: Evidence from zircon U-Pb dating and Lu-Hf isotopes, and whole-rock geochemistry. *Gondwana Research*, 28(2): 800~815.
- Metcalfe I. 2021. Multiple Tethyan ocean basins and orogenic belts in Asia. *Gondwana Research*, 100: 87~130.
- Mikhalsky E V, Sheraton J W. 2011. The Rayner tectonic Province of East Antarctica: Compositional features and geodynamic setting. *Geotectonics*, 45(6): 496~512.
- Morrissey L J, Hand M, Kelsey D E. 2015. Multi-stage metamorphism in the Rayner-Eastern Ghats Terrane: $P-T-t$ constraints from the northern Prince Charles Mountains, east Antarctica. *Precambrian Research*, 267: 137~163.
- Myrow P M, Hughes N C, Searle M P, Fanning C M, Peng S C, Parcha S K. 2009. Stratigraphic correlation of Cambrian-

- Ordovician deposits along the Himalaya: Implications for the age and nature of rocks in the Mount Everest region. *Geological Society of America Bulletin*, 121(3-4): 323~332.
- Myrow P M, Hughes N C, Goode J W, Fanning C M, Williams I S, Peng S C, Bhargava O N, Parcha S K, Pogue K R. 2010. Extraordinary transport and mixing of sediment across Himalayan central Gondwana during the Cambrian-Ordovician. *Geological Society of America Bulletin*, 122(9-10): 1660~1670.
- Pan Guitang, Wang Liqian, Li Rongshe, Yuan Sihua, Ji Wenhua, Yin Fuguang, Zhang Wanping, Wang Baodi. 2012. Tectonic evolution of the Qinghai-Tibet Plateau. *Journal of Asian Earth Sciences*, 53: 3~14.
- Peng Min, Wu Yuanbao, Wang Jing, Jiao Wenfang, Liu Xiaochi, Yang Saishong. 2009. Paleoproterozoic mafic dyke from Kongling terrain in the Yangtze Craton and its implication. *Science Bulletin*, 54(6): 1098~1104.
- Peng Min, Wu Yuanbao, Gao Shan, Zhang Hongfei, Wang Jing, Liu Xiaochi, Gong Hujun, Zhou Lian, Hu Zhaochu, Liu Yongsheng, Yuan Honglin. 2012. Geochemistry, zircon U-Pb age and Hf isotope compositions of Paleoproterozoic aluminous A-type granites from the Kongling terrain, Yangtze Block: Constraints on petrogenesis and geologic implications. *Gondwana Research*, 22(1): 140~151.
- Pullen A, Kapp P, Gehrels G E, Vervoort J D, Ding L. 2008. Triassic continental subduction in central Tibet and Mediterranean-style closure of the Paleo-Tethys Ocean. *Geology*, 36(5): 351~354.
- Reid A J, Wilson C J L, Liu Shun. 2005. Structural evidence for the Permo-Triassic tectonic evolution of the Yidun arc, eastern Tibetan Plateau. *Journal of Structural Geology*, 27(1): 119~137.
- Scherer E, Munker C, Mezger K. 2001. Calibration of the lutetium-hafnium clock. *Science*, 293(5530): 683~687.
- Sláma J, Košler J, Condon D J, Crowley J L, Gerdes A, Hanchar J M, Horstwood S A, Morris G A, Nasdala L, Norberg N, Schaltegger U, Schoene B, Tubrett M N, Whitehouse M J. 2008. Plešovice zircon-A new natural reference material for U-Pb and Hf isotopic microanalysis. *Chemical Geology*, 249(1-2): 1~35.
- Song Xieyan, Zhou Meifu, Cao Zhimin, Robinson P T. 2004. Late Permian rifting of the South China Craton caused by the Emeishan mantle plume? *Journal of the Geological Society*, 161(5): 773~781.
- Su Bingrui, Cui Xiaozhuang, Tian Jingchun, Lai Chun-Kit, Ren Fei, Ren Guangming, Liu Shilei. 2020. Detrital zircon provenance and palaeogeographic implications of the Ediacaran Shigu Group in the Zhongza Terrane, SW China. *International Geology Review*, 62(17): 2105~2124.
- Tian Zhendong. 2020. Geochemical characteristics and tectonic affinity of clastic sedimentary rocks of the Qiasi Group in the Yidun arc. PhD thesis of Chinese Academy of Sciences (in Chinese with English abstract).
- Tian Zhendong, Leng Chengbiao, Zhang Xingchun, Yin Chongjun, Zhang Wei, Guo Jianheng, Chen Lihong. 2018a. Mineralogical and petrogeochemical characteristics of the metamorphic basement of Yidun terrane and their geological implication. *Acta Mineralogical Sinica*, 38(2): 152~165 (in Chinese with English abstract).
- Tian Zhendong, Leng Chengbiao, Zhang Xingchun, Yin Chongjun, Zhang Wei, Guo Jianheng, Tian Feng. 2018b. Mineralogical characteristics of chlorites from Precambrian metamorphic rocks in Yidun magmatic arc of Qinghai-Tibet Plateau and their geological implications. *Journal of Earth Sciences and Environment*, 40(1): 36~48 (in Chinese with English abstract).
- Tian Zhendong, Leng Chengbiao, Zhang Xingchun. 2020. Provenance and tectonic setting of the Neoproterozoic meta-sedimentary rocks at southeastern Tibetan Plateau: Implications for the tectonic affinity of Yidun terrane. *Precambrian Research*, 344: 105736.
- Wang Min, Dai Chuangu, Wang Xuehua, Chen Jianshu, Ma Huizhen. 2011. In-situ zircon geochronology and Hf isotope of muscovite-bearing leucogranites from Fanjingshan, Guizhou Province, and constraints on continental growth of the southern China block. *Earth Science Frontiers*, 18(5): 213~223 (in Chinese with English abstract).
- Wang Wei, Cawood P A, Pandit M K, Zhao Junhong, Zheng Jianping. 2019. No collision between eastern and western Gondwana at their northern extent. *Geology*, 47(4): 308~312.
- Wang Xiaolei, Zhou Jincheng, Griffin W L, Zhao Guochun, Yu Jinhai, Qiu Jiansheng, Zhang Yanjie, Xing Guangfu. 2014. Geochemical zonation across a Neoproterozoic orogenic belt: Isotopic evidence from granitoids and metasedimentary rocks of the Jiangnan orogen, China. *Precambrian Research*, 242: 154~171.
- Wang Xiaolei, Zhou Jincheng, Qiu Jiansheng, Zhang Wenlan, Liu Xiaoming, Zhang Guilin. 2006. LA-ICP-MS U-Pb zircon geochronology of the Neoproterozoic igneous rocks from northern Guangxi, South China: Implications for tectonic evolution. *Precambrian Research*, 145(1-2): 111~130.
- Wang Yuejun, Zhang Aimei, Cawood P A, Fan Weiming, Xu Jifeng, Zhang Guowei, Zhang Yuzhi. 2013. Geochronological, geochemical and Nd-Hf-Os isotopic fingerprinting of an early Neoproterozoic arc-back-arc system in South China and its accretionary assembly along the margin of Rodinia. *Precambrian Research*, 231: 343~371.
- Wang Yuejun, Zhang Yuzhi, Fan Weiming, Geng Hongyan, Zou Heping, Bi Xianwu. 2014. Early Neoproterozoic accretionary assemblage in the Cathaysia Block: Geochronological, Lu-Hf isotopic and geochemical evidence from granitoid gneisses. *Precambrian Research*, 249: 144~161.
- Wiedenbeck M, Alle P, Corfu F, Griffin W, Meier M, Oberli F, Quadri A, Roddick J C, Spiegel W. 1995. Three natural zircon standards for U-Th-Pb, Lu-Hf, trace element and REE analyses. *Geostandards Newsletter*, 19(1): 1~23.
- Xiong Qing, Zheng Jianping, Yu Chunmei, Su Yuping, Tang Huayun, Zhang Zhihai. 2009. Zircon U-Pb age and Hf isotope of Quanyishang A-type granite in Yichang: Signification for the Yangtze continental cratonization in Paleoproterozoic. *Chinese Science Bulletin*, 54(3): 436~446.
- Xu Yajun, Cawood Peter A, Du Yuansheng, Hu Lisha, Yu Wenchao, Zhu Yanhui, Li Wenchao. 2013. Linking South China to northern Australia and India on the margin of Gondwana: Constraints from detrital zircon U-Pb and Hf isotopes in Cambrian strata. *Tectonics*, 32(6): 1547~1558.
- Xu Zhiqin, Yang Jingsui, Hou Zengqian, Zhang Zeming, Zeng Lingsen, Li Haibing, Zhang Jianxin, Li Zhonghai, Ma Xuxuan. 2016. The progress in the study of continental dynamics of the Tibetan Plateau. *Geology in China*, 43(1): 1~42 (in Chinese with English abstract).
- Yao Jinlong, Shu Liangshu, Santosh M, Zhao Guochun. 2014. Neoproterozoic arc-related mafic-ultramafic rocks and syn-collision granite from the western segment of the Jiangnan Orogen, South China: Constraints on the Neoproterozoic assembly of the Yangtze and Cathaysia Blocks. *Precambrian Research*, 243: 39~62.
- Yin A, Harrison T M. 2000. Geologic evolution of the Himalayan-Tibetan orogen. *Annual Review of Earth and Planetary Sciences*, 28(1): 211~280.
- Yu Jinhai, Wang Lijuan, O'Reilly S Y, Griffin W L, Zhang Ming, Li Chunzhong, Shu Liangshu. 2009. A Paleoproterozoic orogeny recorded in a long-lived cratonic remnant (Wuyishan terrane), eastern Cathaysia Block, China. *Precambrian Research*, 174(3-4): 347~363.
- Yuan Honglin, Gao Shan, Dai Mengning, Zong Chunle, Günther D, Fontaine G H, Liu Xiaoming, Diwu Chunrong. 2008. Simultaneous determinations of U-Pb age, Hf isotopes and trace

- element compositions of zircon by excimer laser-ablation quadrupole and multiple collector ICP-MS. *Chemical Geology*, 247 (1-2), 100~118.
- Zhang Aimei, Wang Yuejun, Fan Weiming, Zhang Yuzhi, Yang Joe. 2012. Earliest Neoproterozoic (ca. 1.0 Ga) arc-back-arc basin nature along the northern Yunkai Domain of the Cathaysia Block: Geochronological and geochemical evidence from the metabasite. *Precambrian Research*, 220~221, 217~233.
- Zhang Hongfei, Xu Wangchun, Zong Keqing, Yuan Honglin, Harris N. 2008. Tectonic evolution of metasediments from the Gangdise terrane, Asian plate, eastern Himalayan Syntaxis, Tibet. *International Geology Review*, 50(10), 914~930.
- Zhang Lijuan, Ma Changqian, Wang Lianxun, Shen Zhengbin, Wang Shiming. 2011. Discovery of Paleoproterozoic rapakivi granite on the northern margin of the Yangtze block and its geological significance. *Chinese Science Bulletin*, 56, 306~318.
- Zhao Guochun, Wang Yuejun, Huang Baochun, Dong Yunpeng, Li Sanzhong, Zhang Guowei, Yu Shan. 2018. Geological reconstructions of the East Asian blocks: From the breakup of Rodinia to the assembly of Pangea. *Earth-Science Reviews*, 186, 262~286.
- Zhao Junhong, Zhou Meifu, Yan Danping, Yang Yueheng, Sun Min. 2008. Zircon Lu-Hf isotopic constraints on Neoproterozoic subduction-related crustal growth along the western margin of the Yangtze Block, South China. *Precambrian Research*, 163 (3), 189~209.
- Zhao Junhong, Zhou Meifu, Zheng Jianping, Fang Shiming. 2010. Neoproterozoic crustal growth and reworking of the northwestern Yangtze Block: Constraints from the Xixiang dioritic intrusion, South China. *Lithos*, 120(3), 439~452.
- Zhao Junhong, Zhou Meifu, Zheng Jianping. 2013. Constraints from zircon U-Pb ages, O and Hf isotopic compositions on the origin of Neoproterozoic peraluminous granitoids from the Jiangnan fold belt, South China. *Contributions to Mineralogy and Petrology*, 166(5), 1505~1519.
- Zhao Junhong, Li Qiwei, Liu Hang, Wang Wei. 2018. Neoproterozoic magmatism in the western and northern margins of the Yangtze Block (South China) controlled by slab subduction and subduction-transform-edge-propagator. *Earth-Science Reviews*, 187, 1~18.
- Zhao Kuidong, Jiang Shaoyong, Sun Tao, Chen Weifeng, Ling Hongfei, Chen Peirong. 2013. Zircon U-Pb dating, trace element and Sr-Nd-Hf isotope geochemistry of Paleozoic granites in the Miao'ershan-Yuechengling batholith, South China: Implication for petrogenesis and tectonic-magmatic evolution. *Journal of Asian Earth Sciences*, 74, 244~264.
- Zhao Xinfu, Zhou Meifu, Li Jianwei, Wu Fuyuan. 2008. Association of Neoproterozoic A- and I-type granites in South China: Implications for generation of A-type granites in a subduction-related environment. *Chemical Geology*, 257(1), 1~15.
- Zhao Xinfu, Zhou Meifu, Li Jianwei, Sun Min, Gao Jianfeng, Sun Weihua, Yang Jinhui. 2010. Late Paleoproterozoic to early Mesoproterozoic Dongchuan Group in Yunnan, SW China: Implications for tectonic evolution of the Yangtze Block. *Precambrian Research*, 182(1-2), 57~69.
- Zheng Jianping, Griffin W L, O'Reilly Suzanne Y, Zhang Ming, Pearson Norman, Pan Yuanming. 2006. Widespread Archean basement beneath the Yangtze craton. *Geology*, 34 (6), 417~420.
- Zheng Yongfei, Zhang Shaobing, Zhao Zifu, Wu Yuanbao, Li Xianhua, Li Zhengxiang, Wu Fuyuan. 2007. Contrasting zircon Hf and O isotopes in the two episodes of Neoproterozoic granitoids in South China: Implications for growth and reworking of continental crust. *Lithos*, 96(1-2), 127~150.
- Zhou Guangyan, Wu Yuanbao, Li Long, Zhang Wenxiang, Zheng Jianping, Wang Hao, Yang Saihong. 2018. Identification of ca. 2.65 Ga TTGs in the Yudongzi complex and its implications for the early evolution of the Yangtze Block. *Precambrian Research*, 314, 240~263.
- Zhou Meifu, Yan Danping, Kennedy A, Li Yunqian, Ding Jun. 2002. SHRIMP U-Pb zircon geochronological and geochemical evidence for Neoproterozoic arc-magma along the western margin of the Yangtze Block, South China. *Earth and Planetary Science Letters*, 196(1-2), 51~67.
- Zhou Meifu, Yan Danping, Wang Changliang, Qi Liang, Kennedy A. 2006. Subduction-related origin of the 750 Ma Xuelongbao adakitic complex (Sichuan Province, China): Implications for the tectonic setting of the giant Neoproterozoic magmatic event in South China. *Earth and Planetary Science Letters*, 248(1-2), 286~300.
- Zhou Xueyao, Yu Jinhai, O'Reilly S Y, Griffin W L, Sun Tao, Wang Xiaolei, Tran M, Nguyen D L. 2018. Component variation in the late Neoproterozoic to Cambrian sedimentary rocks of SW China-NE Vietnam, and its tectonic significance. *Precambrian Research*, 308, 92~110.
- Zhu Dichen, Zhao Zhidan, Niu Yaoling, Dilek Y, Mo Xuanxue. 2011. Lhasa terrane in southern Tibet came from Australia. *Geology*, 39(8), 727~730.
- Zhu Weiguang, Zhong Hong, Li Zhengxiang, Bai Zhongjie, Yang Yijin. 2016. SIMS zircon U-Pb ages, geochemistry and Nd-Hf isotopes of ca. 1.0 Ga mafic dykes and volcanic rocks in the Huili area, SW China: Origin and tectonic significance. *Precambrian Research*, 273, 67~89.
- Zhu Yu, Lai Shaocong, Qin Jiangfeng, Zhu Renzhi, Zhang Fangyi, Zhang Zezhong, Zhao Shaowei. 2019a. Neoproterozoic peraluminous granites in the western margin of the Yangtze Block, South China: Implications for the reworking of mature continental crust. *Precambrian Research*, 333, 105443.
- Zhu Yu, Qin Jiangfeng, Zhu Renzhi, Zhang Fangyi, Zhang Zezhong, Gan Baoping. 2019b. Petrogenesis and geodynamic implications of Neoproterozoic gabbro-diorites, adakitic granites, and A-type granites in the southwestern margin of the Yangtze Block, South China. *Journal of Asian Earth Sciences*, 183, 103977.

参 考 文 献

- 董昕, 张泽明, 王金丽, 赵国春, 刘峰, 王伟, 于飞. 2009. 青藏高原拉萨地体南部林芝岩群的物质来源与形成年代: 岩石学与锆石 U-Pb 年代学. *岩石学报*, 25(7), 1678~1694.
- 杜其良. 1986. 四川木里水洛地区前寒武纪地层的发现及其初步划分. *成都地质学院学报*(1), 31~49.
- 龚日祥, 颜铁增, 余心起, 华锡宏, 张志芳. 2009. 论浙江平水群的划分和地质时代. *现代地质*, 23(02), 238~245.
- 田振东. 2020. 义敦岛弧恰斯群碎屑沉积岩地球化学特征及构造亲缘性研究. *中国科学院大学博士学位论文*.
- 田振东, 冷成彪, 张兴春, 尹崇军, 张伟, 郭剑衡, 陈利红. 2018a. 义敦地体变质基底地球化学特征与地质意义. *矿物学报*, 38 (2), 152~165.
- 田振东, 冷成彪, 张兴春, 尹崇军, 张伟, 郭剑衡, 田丰. 2018b. 青藏高原义敦岩浆弧前寒武系变质岩绿泥石矿物学特征及其地质意义. *地球科学与环境学报*, 40(1), 36~48.
- 许志琴, 杨经绥, 侯增谦, 张泽明, 曾令森, 李海兵, 张建新, 李忠海, 马绪宣. 2016. 青藏高原大陆动力学研究若干进展. *中国地质*, 43(1), 1~42.

Early Paleozoic tectonic framework of the Yidun Terrane, eastern Tibetan Plateau: Constraints from detrital zircon U-Pb-Hf isotopic compositions

TIAN Zhendong¹⁾, LENG Chengbiao^{2, 3)}, GUO Jianheng⁴⁾, ZHANG Xingchun^{*1)},
TIAN Feng⁵⁾, MA Ronglin¹⁾

1) State Key Laboratory of Ore Deposit Geochemistry, Institute of Geochemistry,

Chinese Academy of Sciences, Guiyang, Guizhou 550081, China;

2) State Key Laboratory of Nuclear Resources and Environment, East China University of
Technology, Nanchang, Jiangxi 330013, China;

3) School of Earth Sciences, East China University of Technology, Nanchang, Jiangxi 330013, China;

4) Suzhou Institute of Economics and Trade, Suzhou, Jiangsu 215009, China;

5) Yeqin Geological Team of Hubei Geological Bureau, Shiyan, Hubei 442000, China

* Corresponding author: zhangxingchun@mail.vip.ac.cn

Abstract

The Yidun Terrane, located in the eastern Tibetan Plateau, is a key area to study the tectonic evolution of the Tibetan Plateau and the Paleo-Tethys. To date, its paleogeographic position and possible tectonic evolution during the early Paleozoic remain unclear. Detrital zircons from siliciclastic rocks record a wealth of information about their source region and have been widely used to unravel sedimentary provenance and paleogeographic construction. In this study, we conducted detrital zircon in-situ U-Pb dating and Hf isotope analysis of three lower Paleozoic meta-sedimentary rocks in the terrane. The results show that these samples have multi-peak detrital zircon age patterns, their U-Pb ages are mainly grouped into ca.2535~2350 Ma, ca.1000~900 Ma, ca.890~750 Ma, and ca.590~520 Ma, and their corresponding $\epsilon_{\text{Hf}}(t)$ values are -8.8 to 13.1, -11.8 to 10.0, -20.1 to 12.6, and -27.6 to 6.1, respectively. Combining these results with previous studies, we consider that the ca.2535~2350 Ma and ca.890~750 Ma detrital zircons were predominantly sourced from the nearby Songpan-Ganze Terrane and South China Block, whereas the ca.1000~900 Ma and ca.590~520 Ma detrital zircons were likely derived from the Rayner-Eastern Ghats, Prydz-Darling, and Kuunga orogens in the East Gondwana. By comparing the difference in sedimentary provenance between the lower Paleozoic and Neoproterozoic siliciclastic rocks in the Yidun Terrane, as well as those lower Paleozoic sedimentary rocks in the nearby terranes, we suggest that the Yidun Terrane was probably collaged to the India Block during late Ediacaran to early Cambrian (ca.570~520), and became part of the Gondwana supercontinent. In the early Paleozoic, the Yidun Terrane was located on the northern margin of the East Gondwana, adjacent to the Qiangtang and Tethyan Himalaya terranes.

Key words: Yidun terrane; Qiasi Group; sedimentary provenance; detrital zircon; tectonic evolution